

Joint Power Allocation and Passive Beamforming Design for IRS-Assisted Physical-Layer Service Integration

Boyu Ning, *Student Member, IEEE*, Zhi Chen, *Senior Member, IEEE*,
Zhongbao Tian, *Student Member, IEEE*, and Shaoqian Li, *Fellow, IEEE*

Abstract

Intelligent reflecting surface (IRS) has emerged as an appealing solution to enhance the wireless communication performance by reconfiguring the wireless propagation environment. In this paper, we propose to apply IRS to the physical-layer service integration (PHY-SI) system, where a single-antenna access point (AP) integrates two sorts of service messages, i.e., multicast message and confidential message, via superposition coding to serve multiple single-antenna users. Our goal is to optimize the power allocation (for transmitting different messages) at the AP and the passive beamforming at the IRS to maximize the achievable secrecy rate region. To this end, we formulate this problem as a bi-objective optimization problem, which is shown equivalent to a secrecy rate maximization problem subject to the constraints on the quality of multicast service. Due to the non-convexity of this problem, we propose two customized algorithms to obtain its high-quality suboptimal solutions, thereby approximately characterizing the secrecy rate region. The resulting performance gap with the globally optimal solution is analyzed. Furthermore, we provide theoretical analysis to unveil the impact of IRS beamforming on the performance of PHY-SI. Numerical results demonstrate the advantages of leveraging IRS in improving the performance of PHY-SI and also validate our theoretical analysis.

Index Terms

Intelligent reflecting surface, physical layer service integration, multicasting, wiretap channel, secrecy rate region.

This work was supported in part by the National Key R&D Program of China under Grant 2018YFB1801500.

The authors are with National Key Laboratory of Science and Technology on Communications, University of Electronic Science and Technology of China, Chengdu 611731, China (e-mails: boydning@outlook.com; chen zhi@uestc.edu.cn; Vincent11231@outlook.com; lsq@ uestc.edu.cn).

I. INTRODUCTION

Recently, intelligent reflecting surface (IRS) has emerged as an appealing candidate for future wireless communications due to its low hardware cost and energy consumption [1]–[3]. Specifically, IRS is a planar array consisting of massive reflecting elements, each being able to passively reflect the incident wireless signal by adjusting its phase shift (PS). By controlling the PSs at IRS, the reflected signals of different elements can be added/counteracted in intended/unintended directions, thus resulting in a programmable and controllable wireless environment. In view of this advantage, both academia and industry have been exploring the performance optimization in different IRS-assisted systems. For example, in a multi-input single-output (MISO) IRS-assisted system, different optimization targets, e.g., transmit power minimization [4], weighted sum-rate maximization [5], and energy efficiency maximization [6], etc., have been investigated by jointly optimizing the active beamforming at the access point (AP) and PSs (or passive beamforming) at IRS. In the more general and challenging multi-input multi-output (MIMO) IRS-assisted system, the authors in [7]–[9] have proposed some suboptimal algorithms, e.g., sum-path-gain maximization approach [7], alternating optimization (AO)-based method [8], and manifold optimization (MO)-based algorithm [9], etc., to maximize the channel capacity. As a further advance, the authors in [10] focused on a multi-cell IRS-assisted MIMO network and proposed a block coordinate descent (BCD) algorithm to maximize the weighted sum-rate of all users [10].

On the other hand, physical-layer security (PLS) is also a critical issue in wireless communications. Exploiting IRS to improve the performance of PLS has been widely studied in the literature recently. For example, in the case with one legitimate user and one eavesdropper, [11]–[15] have proposed different algorithms, e.g., the alternating direction method of multipliers (ADMM) algorithm [11], semidefinite relaxation (SDR) [12], and majorization-minimization (MM) method [13], to jointly optimize the active and passive beamforming for maximizing the minimum-secrecy-rate. Furthermore, the authors in [14] considered a more general broadcast system with multiple legitimate users and multiple eavesdroppers and proposed an alternating optimization (with path-following procedures) algorithm to maximize the secrecy rate. Besides, it was revealed in [15] that emitting artificial noise (AN) is an effective means for enhancing the secrecy rate in IRS-assisted systems. It is worth noting that in [11]–[15], it is assumed that each legitimate user only requests the confidential message while other users who do not request this message are treated as eavesdroppers.

Nevertheless, in practice, all of these users may order assorted services at the same time. For example, both confidential and public (e.g., multicast) messages may coexist by applying the emerging physical-layer service integration (PHY-SI) technique, which integrates confidential and multicast messages via superposition coding for one-time transmission, so as to improve the spectral efficiency. In fact, the concept of PHY-SI can be traced back to Csiszár and Körner's seminal work [16] for a discrete memoryless broadcast channel. This work was later extended to the general MIMO systems [18] and bidirectional relay networks [19]. In PHY-SI, each user first decodes the common multicast message and the legitimate user further decodes the confidential message by subtracting the decoded multicast message. As such, a basic problem in PHY-SI lies in how to reconcile the trade-off between maximizing the quality of the confidential service (or secrecy rate) and that of the multicast service (or the minimum achievable rate among all users when decoding the multicast message, referred to as multicast rate in the sequel of this paper) [17]. This can be formulated as a bi-objective secrecy rate region maximization problem. To solve this problem, the authors in [18] proposed a re-parameterization method to find all of its Pareto optimal solutions, i.e., the boundary points of the secrecy rate region. An alternative approach is by reformulating this bi-objective optimization problem as a secrecy rate maximization problem yet subject to an additional constraint on the quality of multicast service (QoMS). By traversing the desired multicast rate included in the QoMS constraint, all Pareto optimal solutions can be derived [20]. Moreover, the authors in [21] revealed that emitting AN may not always bring performance gain in PHY-SI as it results in co-channel interference to the multicast message, which is fundamentally different from PLS. Along with the advent of IRS, it is an interesting problem to study whether IRS helps enhance the performance of PHY-SI. However, to the best of our knowledge, this problem has not been studied yet.

To fill in this gap, we consider this secrecy rate region maximization problem in a multi-user single-input single-output (SISO) IRS-assisted system, where all users have ordered the multicast service, while one user further orders the confidential service. Thus, in decoding its confidential message, all other users are treated as eavesdroppers. It is worth noting that as compared to the conventional PHY-SI without IRS, maximizing the secrecy rate region is a much more challenging problem even in the SISO case. This is due to the non-convex unit-modulus constraints on the IRS passive beamforming, which is coupled in the secrecy rate and multicast rate. Our goal is to optimize the power allocation (for transmitting the multicast and confidential messages) at the AP and the IRS passive beamforming to find all Pareto optimal

solutions. To this end, we first consider a two-user system (thus with only a single eavesdropper). Specifically, we show that the bi-objective optimization problem is equivalent to a secrecy rate maximization problem subject to QoMS constraints. However, this equivalent problem is still non-convex. To tackle this challenge, we propose a Charnes-Cooper transformation (CCT)-based algorithm to approximately solve it via the SDR technique. Furthermore, we show that the optimal power allocation ratio can be obtained in closed-form with any given passive beamforming. By leveraging this fact, we also proposed a weighted sum covariance matrix (WSCM)-based algorithm with lower complexity to solve the considered problem. Next, we extend the above algorithms to accommodate the general multi-user/eavesdropper scenario and characterize the performance gap to the globally optimal solution. To draw useful insights, we perform theoretical analysis to unveil the impact of IRS passive beamforming on the performance of PHY-SI versus that without IRS. Numerical results demonstrate that the performance of our proposed algorithms can yield near-optimal performance. The results also reveal that the secrecy rate region can be significantly enlarged by leveraging IRS compared to the scheme without IRS. In particular, by equipping the IRS with sufficient number of elements, the number of users who can achieve positive secrecy rate can be increased significantly.

The rest of this paper is organized as follows. Section II introduces the system model and the problem formulation. In Sections III and IV, efficient algorithms are proposed to solve the formulated problems in the two-user and multi-user cases, respectively. Section V provides the theoretical analysis on the IRS-assisted PHY-SI. Section V presents the numerical results to evaluate the efficacy of our proposed algorithms. Finally, we conclude the paper in Section VI.

Notation: We use small normal face for scalars, small bold face for vectors, and capital bold face for matrices. $\text{Tr}(\cdot)$, $\text{rank}(\cdot)$, and $|\cdot|$ represent the trace, rank, and modulus of a matrix, respectively. The superscript $\{\cdot\}^*$ and $\{\cdot\}^H$ denote the conjugate and Hermitian transpose. $\mathbf{a}(n)$ represents the n th element of \mathbf{a} . $\text{diag}(\cdot)$ denotes a diagonal matrix whose diagonal elements are given by its argument. $\mathcal{CN}(\mu, \sigma^2)$ means circularly symmetric complex Gaussian (CSCG) distribution with mean of μ and variance of σ^2 . \mathbf{I} denotes the identity matrix. \mathbb{K} represents a proper cone, and \mathbb{K}^* represents a dual cone associated with \mathbb{K} .

II. SYSTEM MODEL AND PROBLEM FORMULATION

We consider an IRS-assisted communication system as depicted in Fig. 1, where a single-antenna AP serves K single-antenna users, with the assistance of an IRS equipped with N passive

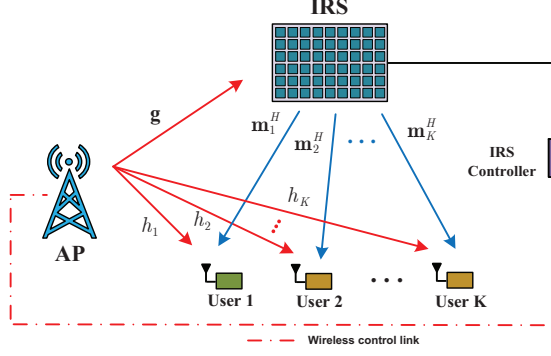


Fig. 1. An IRS-assisted PHY-SI system.

PSs and installed on a nearby wall. We assume that all the users have requested a multicast service and user 1 further requests a confidential service. As such, the other users serve as potential internal eavesdroppers which are able to eavesdrop the confidential information intended for user 1. For ease of exposition, we define $\mathcal{K} \triangleq \{1, 2, \dots, K\}$ and $\mathcal{E} \triangleq \mathcal{K}/\{1\}$ to represent the index set of all users and that of eavesdroppers, respectively. In PHY-SI, the AP transmits the superposition of the confidential message $s_c \sim \mathcal{CN}(0, 1)$ and the multicast message $s_m \sim \mathcal{CN}(0, 1)$, denoted as

$$x = \sqrt{\alpha}s_c + \sqrt{\beta}s_m, \quad (1)$$

where α and β represent the transmit power allocated to the confidential message and multicast message, respectively. To characterize the theoretical limit of the considered system, we assume that the channel state information (CSI) on all links involved are available at the AP and can be sent to the IRS controller for tuning the IRS's PSs. In practice, this channel knowledge can be obtained by using some customized channel estimation schemes for IRS-aided wireless communications (see [22]–[24]). In addition, we consider the quasi-static block fading channels, i.e., all channels involved remain constant within the considered fading block. Let $\{h_k\}_{k=1}^K \in \mathbb{C}$, $\{\mathbf{m}_k^H\}_{k=1}^K \in \mathbb{C}^{1 \times N}$, and $\mathbf{g} \in \mathbb{C}^{N \times 1}$ denote the baseband equivalent channels of AP-user k link, IRS-user k link, and AP-IRS link, respectively. With the IRS, the transmitted signal via \mathbf{g} can be dynamically altered by its N PSs, denoted as $\mathbf{\Theta} = \text{diag}(e^{j\theta_1}, e^{j\theta_2}, \dots, e^{j\theta_N})$, and then reflected to the users via channels $\{\mathbf{m}_k^H\}_{k=1}^K$, where $j = \sqrt{-1}$ is an imaginary unit and $\theta_i \in [0, 2\pi)$, $i = 1, 2, \dots, N$ is PS in the i -th reflecting element of the IRS. The overall received signal at user k from both AP-user link and AP-IRS-user link can be expressed as [18]

$$y_k = \sqrt{\alpha}(\mathbf{m}_k^H \mathbf{\Theta} \mathbf{g} + h_k)s_c + \sqrt{\beta}(\mathbf{m}_k^H \mathbf{\Theta} \mathbf{g} + h_k)s_m + n_k, \quad k \in \mathcal{K}, \quad (2)$$

where $n_k \sim \mathcal{CN}(0, \sigma_k^2)$ is the zero-mean additive Gaussian noise with power σ_k^2 . Here, we ignore the signals reflected by the IRS more than once due to the severe path-loss. Denote R_c and R_m as the achievable rates of the confidential message and the multicast message, respectively. Given the total power constraint $\alpha + \beta \leq P$, the secrecy rate region $C_s(\{h_k\}_{k=1}^K, \{\mathbf{m}_k^H\}_{k=1}^K, \mathbf{g}, P)$ is defined as a set of non-negative rate pairs (R_m, R_c) satisfying [18]

$$R_m \leq \min_{k \in \mathcal{K}} \log \left(1 + \frac{\beta |\mathbf{m}_k^H \mathbf{\Theta} \mathbf{g} + h_k|^2}{\sigma_k^2 + \alpha |\mathbf{m}_k^H \mathbf{\Theta} \mathbf{g} + h_k|^2} \right), \quad (3a)$$

$$R_c \leq \log \left(1 + \frac{\alpha |\mathbf{m}_1^H \mathbf{\Theta} \mathbf{g} + h_1|^2}{\sigma_1^2} \right) - \max_{k \in \mathcal{E}} \log \left(1 + \frac{\alpha |\mathbf{m}_k^H \mathbf{\Theta} \mathbf{g} + h_k|^2}{\sigma_k^2} \right). \quad (3b)$$

It is observed from (3) that all users first decode the multicast message by treating the confidential message as noise. By removing the decoded multicast message, user 1 then decodes the confidential message without interference from the multicast message.

In this work, we focus on characterizing the secrecy rate region C_s in the presence of an assisted IRS. This is equivalent to solving a bi-objective optimization problem below with cone $\mathbb{K} = \mathbb{K}^* = \mathbb{R}_+^2$, i.e.,

$$(P1) : \max_{\alpha, \beta, \mathbf{v}, R_m, R_c} (\text{w.r.t. } \mathbb{R}_+^2) (R_m, R_c) \quad (4a)$$

$$\text{s.t. } \min_{k \in \mathcal{K}} \log \left(1 + \frac{\beta |\mathbf{m}_k^H \text{diag}(\mathbf{v}^*) \mathbf{g} + h_k|^2}{\sigma_k^2 + \alpha |\mathbf{m}_k^H \text{diag}(\mathbf{v}^*) \mathbf{g} + h_k|^2} \right) \geq R_m, \quad (4b)$$

$$\min_{k \in \mathcal{E}} \log \frac{\sigma_1^2 \sigma_k^2 + \sigma_k^2 \alpha |\mathbf{m}_1^H \text{diag}(\mathbf{v}^*) \mathbf{g} + h_1|^2}{\sigma_1^2 \sigma_k^2 + \sigma_1^2 \alpha |\mathbf{m}_k^H \text{diag}(\mathbf{v}^*) \mathbf{g} + h_k|^2} \geq R_c, \quad (4c)$$

$$\alpha + \beta \leq P, \quad \alpha \geq 0, \quad \beta \geq 0, \quad |\mathbf{v}(i)| = 1, \quad i = 1, 2, \dots, N. \quad (4d)$$

where $\mathbf{v} = [e^{j\theta_1}, e^{j\theta_2}, \dots, e^{j\theta_{N_r}}]^H$ denotes the PS vector at the IRS, i.e., $\mathbf{\Theta} = \text{diag}(\mathbf{v}^*)$. The constraint in (4c) is derived by reformulating (3b). For (P1), we have the following proposition.

Proposition 1. (P1) is feasible if $\left| \sum_{i=1}^N |\mathbf{m}_1(i)| |\mathbf{g}(i)| + h_1 \right|^2 \geq \max_k \frac{\sigma_1^2}{\sigma_k^2} \left| \sum_{i=1}^N |\mathbf{m}_k(i)| |\mathbf{g}(i)| + h_k \right|^2$, and (P1) is infeasible if there exists a k satisfying $\left| \sum_{i=1}^N |\mathbf{m}_1(i)| |\mathbf{g}(i)| + h_1 \right|^2 \leq \frac{\sigma_1^2 |h_k|^2}{\sigma_k^2}$.

Proof. See Appendix A. □

Note that (P1) is a bi-objective optimization problem. Any Pareto optimal solution to this problem is a boundary point of C_s . However, due to the non-convex constraints with regard to (w.r.t.) the coupled variables and the unit-modulus constraint on \mathbf{v} , (P1) is challenging to be solved optimally. To characterize the secrecy rate region, next, we propose an approach to find all (approximate) Pareto optimal points of (P1).

III. TWO-USER SYSTEM

In this section, we first consider a two-user system, i.e., $K = 2$.

A. An Equivalent Scalar Maximization Problem of (P1)

In order to find all the Pareto optimal solutions to (P1), we formulate an equivalent scalar maximization problem of (P1) by fixing one entry of (R_m, R_c) and maximizing the other one. Specifically, we fix the variable R_m as a constant $r_m \in [0, r_m^{\max}]$, where r_m^{\max} is the maximum achievable multicast rate. As such, maximizing the vector (R_m, R_c) reduces to maximizing R_c , which is equivalent to the following problem,

$$(P2) : \overline{R}_c(r_m) = \max_{\alpha, \beta, \mathbf{v}} \left[\log \frac{\sigma_1^2 \sigma_2^2 + \sigma_2^2 \alpha |\mathbf{m}_1^H \text{diag}(\mathbf{v}^*) \mathbf{g} + h_1|^2}{\sigma_1^2 \sigma_2^2 + \sigma_1^2 \alpha |\mathbf{m}_2^H \text{diag}(\mathbf{v}^*) \mathbf{g} + h_2|^2} \right]^+ \quad (5a)$$

$$\text{s.t. } \log \left(1 + \frac{\beta |\mathbf{m}_1^H \text{diag}(\mathbf{v}^*) \mathbf{g} + h_1|^2}{\sigma_1^2 + \alpha |\mathbf{m}_1^H \text{diag}(\mathbf{v}^*) \mathbf{g} + h_1|^2} \right) \geq r_m, \quad (5b)$$

$$\log \left(1 + \frac{\beta |\mathbf{m}_2^H \text{diag}(\mathbf{v}^*) \mathbf{g} + h_2|^2}{\sigma_2^2 + \alpha |\mathbf{m}_2^H \text{diag}(\mathbf{v}^*) \mathbf{g} + h_2|^2} \right) \geq r_m, \quad (5c)$$

$$\alpha + \beta \leq P, \quad \alpha \geq 0, \quad \beta \geq 0, \quad |\mathbf{v}(i)| = 1, \quad i = 1, 2, \dots, N. \quad (5d)$$

(P2) can be interpreted as finding the maximum achievable secrecy rate under the QoMS constraint. By following the Theorem 1 given in [20], it is easy to prove that $(r_m, \overline{R}_c(r_m))$ must be a Pareto optimal solution to (P1), i.e., a boundary point of C_s . In addition, some interesting properties w.r.t. (P2) are listed as follows.

- When $r_m = 0$, the QoMS constraint is inactive and (P2) becomes a conventional secrecy rate maximization problem with $\overline{R}_c(0) = r_c^{\max}$, where r_c^{\max} is the maximum achievable secrecy rate in our considered system.
- When r_m increases, the feasible region of (P2) will be shrank. Thus, the optimum $\overline{R}_c(r_m)$ is monotonically non-increasing with r_m .
- When $r_m = r_m^{\max}$, all transmit power must be allocated to transmit the multicast message for achieving the maximum multicast rate, i.e., $\beta = P$ and $\alpha = 0$, with $\overline{R}_c(r_m^{\max}) = 0$.

It follows from the above properties that with increasing r_m from 0 to r_m^{\max} , the optimal value $\overline{R}_c(r_m)$ of (P2) will decrease from r_c^{\max} to 0. Thus, the two endpoints of the region C_s are given by $(0, r_c^{\max})$ and $(r_m^{\max}, 0)$, respectively. As a result, by varying the parameter r_m within $[0, r_m^{\max}]$, all the Pareto optimal solutions to (P1) can be obtained by solving (P2).

B. An Upper Bound on the Maximum Multicast Rate

However, it is generally difficult to obtain r_m^{\max} since maximizing the multicast rate is also a challenging optimization problem, i.e.,

$$\begin{aligned} (\text{P3}) : r_m^{\max} &= \max_{\beta, \mathbf{v}} \min_{k=1,2} \log \left(1 + \frac{\beta}{\sigma_k^2} |\mathbf{m}_k^H \text{diag}(\mathbf{v}^*) \mathbf{g} + h_k|^2 \right) \\ \text{s.t. } &\beta \leq P, \beta \geq 0, |\mathbf{v}(i)| = 1, i = 1, 2, \dots, N. \end{aligned} \quad (6)$$

Thus, we aim to find an upper bound on r_m^{\max} , denoted as r_m^{up} , by solving (P3) via the SDR technique. By varying the parameter r_m within $[0, r_m^{\text{up}}]$, we can still find all the Pareto optimal points by solving (P2). In particular, when $r_m \in [r_m^{\max}, r_m^{\text{up}}]$, there is no solution to (P2). To reformulate (P3) into an SDR problem, we first rewrite its objective function as an equivalent form. Specifically, by using the equality $\mathbf{m}_k^H \text{diag}(\mathbf{v}^*) = \mathbf{v}^H \text{diag}(\mathbf{m}_k^*)$, we have

$$\begin{aligned} &\log \left(1 + \frac{\beta}{\sigma_k^2} |\mathbf{m}_k^H \text{diag}(\mathbf{v}^*) \mathbf{g} + h_k|^2 \right) \\ &= \log \left[1 + \frac{\beta}{\sigma_k^2} (\mathbf{v}^H \text{diag}(\mathbf{m}_k^*) \mathbf{g} \mathbf{g}^H \text{diag}(\mathbf{m}_k) \mathbf{v} \right. \\ &\quad \left. + \mathbf{v}^H \text{diag}(\mathbf{m}_k^*) \mathbf{g} h_k^* + h_k \mathbf{g}^H \text{diag}(\mathbf{m}_k) \mathbf{v} + h_k^* h_k) \right] \\ &= \log \left(1 + \frac{\beta}{\sigma_k^2} \mathbf{z}^H \mathbf{T}_k \mathbf{z} \right) \end{aligned} \quad (7)$$

where $\mathbf{z} = [t \cdot \mathbf{v}^H, t]^H$ and t is an introduced auxiliary variable satisfying $|t| = 1$. The matrix \mathbf{T}_k is given by

$$\mathbf{T}_k = \begin{bmatrix} \text{diag}(\mathbf{m}_k^*) \mathbf{g} \mathbf{g}^H \text{diag}(\mathbf{m}_k) & \text{diag}(\mathbf{m}_k^*) \mathbf{g} h_k^* \\ h_k \mathbf{g}^H \text{diag}(\mathbf{m}_k) & h_k^* h_k \end{bmatrix}, \quad k = 1, 2. \quad (8)$$

By noting that $\mathbf{z}^H \mathbf{T}_k \mathbf{z} = \text{Tr}(\mathbf{z} \mathbf{z}^H \mathbf{T}_k)$, we define $\mathbf{Z} = \mathbf{z} \mathbf{z}^H$ which satisfies $\mathbf{Z} \succeq 0$ and $\text{rank}(\mathbf{Z}) = 1$. It is obvious that the maximum multicast rate is achieved when setting $\beta = P$. By relaxing the rank one constraint and introducing a slack variable τ , (P3) becomes a convex optimization problem, i.e.,

$$\begin{aligned} (\hat{\text{P3}}) : r_m^{\text{up}} &= \max_{\mathbf{Z}, \tau} \tau \\ \text{s.t. } &\text{Tr} \left(\frac{P}{\sigma_1^2} \mathbf{Z} \mathbf{T}_1 \right) \geq 2^\tau - 1, \quad \text{Tr} \left(\frac{P}{\sigma_2^2} \mathbf{Z} \mathbf{T}_2 \right) \geq 2^\tau - 1, \\ &\text{Tr}(\mathbf{Z} \mathbf{E}_i) = 1, \quad i = 1, 2, \dots, N+1, \quad \mathbf{Z} \succeq \mathbf{0}. \end{aligned} \quad (9)$$

The relaxed problem ($\hat{\text{P3}}$) is a convex semidefinite program (SDP), thus can be optimally solved by the interior-point method or CVX [25]. Generally, due to the relaxed feasible region, the solution to ($\hat{\text{P3}}$) may not be rank one and thus we have $r_m^{\text{up}} \geq r_m^{\max}$.

C. Proposed Solution to (P2)

Given $r_m \in [0, r_m^{\text{up}}]$, we aim to find all Pareto optimal solutions to (P1) by solving (P2). However, (P2) is a nonconvex optimization problem. In the sequel, we propose a CCT-based algorithm to tackle it for characterizing the secrecy rate region.

Remark 1. When $\bar{R}_c(0) = 0$, the secrecy rate region C_s reduces to a line segment on the axis of the multicast rate, i.e., $C_s = \{(0, R_m) | R_m \in [0, r_m^{\text{max}}]\}$. In this case, our considered problem is degraded into the multicast rate maximization problem, i.e., (P3).

Remark 1 implies that (P2) is trivial when $\bar{R}_c(0) = 0$, thus we assume $\bar{R}_c(0) > 0$ in this paper, which is equivalent to the following condition,

$$\frac{|\mathbf{m}_1^H \text{diag}(\mathbf{v}^*)\mathbf{g} + h_1|^2}{\sigma_1^2} > \frac{|\mathbf{m}_2^H \text{diag}(\mathbf{v}^*)\mathbf{g} + h_2|^2}{\sigma_2^2}. \quad (10)$$

Define a function $f(x) = \log[1 + \beta x / (1 + \alpha x)]$ and it is easy to verify that $f(x)$ is monotonically increasing with x . Note that the left hand sides (LHSs) of (5b) and (5c) can be expressed as $f(|\mathbf{m}_1^H \text{diag}(\mathbf{v}^*)\mathbf{g} + h_1|^2 / \sigma_1^2)$ and $f(|\mathbf{m}_2^H \text{diag}(\mathbf{v}^*)\mathbf{g} + h_2|^2 / \sigma_2^2)$, respectively. Thus, (10) implies that the former must be greater than the latter. Hence, constraint (5b) is redundant and can be discarded in the optimization. Next, we further simplify (P2) based on the facts below.

- 1) We ignore the logarithmic function due to the monotonicity property.
- 2) The total transmit power constraint is tight when the maximum secrecy rate is achieved, i.e., $\alpha + \beta = P$.
- 3) Similar to the reformulation in (7), we have the following equivalent relations,

$$\frac{\sigma_1^2 \sigma_2^2 + \sigma_2^2 \alpha |\mathbf{m}_1^H \text{diag}(\mathbf{v}^*)\mathbf{g} + h_1|^2}{\sigma_1^2 \sigma_2^2 + \sigma_1^2 \alpha |\mathbf{m}_2^H \text{diag}(\mathbf{v}^*)\mathbf{g} + h_2|^2} = \frac{\sigma_1^2 \sigma_2^2 + \sigma_2^2 \alpha \text{Tr}(\mathbf{Z}\mathbf{T}_1)}{\sigma_1^2 \sigma_2^2 + \sigma_1^2 \alpha \text{Tr}(\mathbf{Z}\mathbf{T}_2)} = \frac{\text{Tr}[\mathbf{Z}(\frac{\sigma_1^2 \sigma_2^2}{N+1} \mathbf{I} + \sigma_2^2 \alpha \mathbf{T}_1)]}{\text{Tr}[\mathbf{Z}(\frac{\sigma_1^2 \sigma_2^2}{N+1} \mathbf{I} + \sigma_1^2 \alpha \mathbf{T}_2)]}, \quad (11)$$

$$\frac{\beta |\mathbf{m}_2^H \boldsymbol{\Theta} \mathbf{g} + h_2|^2}{\sigma_2^2 + \alpha |\mathbf{m}_2^H \boldsymbol{\Theta} \mathbf{g} + h_2|^2} = \frac{(P - \alpha) \text{Tr}(\mathbf{Z}\mathbf{T}_2)}{\sigma_2^2 + \alpha \text{Tr}(\mathbf{Z}\mathbf{T}_2)} = \frac{\text{Tr}[(P - \alpha) \mathbf{Z}\mathbf{T}_2]}{\text{Tr}[\mathbf{Z}(\frac{\sigma_2^2}{N+1} \mathbf{I} + \alpha \mathbf{T}_2)]}. \quad (12)$$

Based on the above facts, solving (P2) is equivalent to solving the following problem (P4),

$$\begin{aligned} \text{(P4)} : \quad & 2\bar{R}_c(r_m) = \max_{\alpha, \mathbf{Z}} \frac{\text{Tr}[\mathbf{Z}(\frac{\sigma_1^2 \sigma_2^2}{N+1} \mathbf{I} + \sigma_2^2 \alpha \mathbf{T}_1)]}{\text{Tr}[\mathbf{Z}(\frac{\sigma_1^2 \sigma_2^2}{N+1} \mathbf{I} + \sigma_1^2 \alpha \mathbf{T}_2)]} \\ & \text{s.t.} \quad \frac{\text{Tr}[(P - \alpha) \mathbf{Z}\mathbf{T}_2]}{\text{Tr}[\mathbf{Z}(\frac{\sigma_2^2}{N+1} \mathbf{I} + \alpha \mathbf{T}_2)]} \geq 2^{r_m} - 1, \\ & \quad \text{Tr}(\mathbf{Z}\mathbf{E}_i) = 1, \quad i = 1, 2, \dots, N+1, \\ & \quad \text{rank}(\mathbf{Z}) = 1, \quad \mathbf{Z} \succeq \mathbf{0}, \quad \alpha \geq 0, \quad P - \alpha \geq 0. \end{aligned} \quad (13)$$

Problem (P4) is a fractional programming problem. To solve it, we propose an efficient approach to transform this problem into a more tractable form by applying the CCT, i.e.,

$$\mathbf{Z} = \mathbf{Y}/\xi, \quad \xi > 0. \quad (14)$$

Meanwhile, we relax the rank one constraint and (P4) is reduced to

$$\begin{aligned} (\hat{\text{P4}}) \quad & \max_{\alpha, \mathbf{Y}, \xi} \text{Tr}[\mathbf{Y}(\frac{\sigma_1^2 \sigma_2^2}{N+1} \mathbf{I} + \sigma_2^2 \alpha \mathbf{T}_1)] \\ \text{s.t.} \quad & \text{Tr}[\mathbf{Y}(\frac{\sigma_1^2 \sigma_2^2}{N+1} \mathbf{I} + \sigma_1^2 \alpha \mathbf{T}_2)] = 1, \\ & \text{Tr} \left\{ \mathbf{Y} \left[(P - \alpha 2^{r_m}) \mathbf{T}_2 - \frac{(2^{r_m} - 1) \sigma_2^2}{N+1} \mathbf{I} \right] \right\} \geq 0, \\ & \text{Tr}(\mathbf{Y} \mathbf{E}_i) = \xi, \quad i = 1, 2, \dots, N+1, \\ & \mathbf{Y} \succeq \mathbf{0}, \quad \alpha \geq 0, \quad P - \alpha \geq 0, \quad \xi > 0. \end{aligned} \quad (15)$$

Note that $(\hat{\text{P4}})$ is a coordinate-wise convex optimization problem w.r.t α and $\{\mathbf{Y}, \xi\}$. A straightforward approach to solve it is by using the alternating optimization (AO), i.e., optimizing α with fixed $\{\mathbf{Y}, \xi\}$ and optimizing $\{\mathbf{Y}, \xi\}$ with fixed α in an alternate manner. However, as the objective function of $(\hat{\text{P4}})$ is not jointly convex w.r.t $\{\alpha, \mathbf{Y}, \xi\}$, AO generally can only yield a local optimal solution. To improve over AO, by noting $\alpha \in [0, P]$, the globally optimal solution to $(\hat{\text{P4}})$ can be obtained via a one dimensional search over α whilst optimizing $\{\mathbf{Y}, \xi\}$ in every search. In particular, $(\hat{\text{P4}})$ is an SDP with fixed α and the optimal α should be chosen as the one that leads to the maximum objective value of $(\hat{\text{P4}})$.

Generally, the globally optimal solution $\{\alpha, \mathbf{Y}, \xi\}$ to $(\hat{\text{P4}})$ may not lead to a feasible PS vector \mathbf{v} to (P2) unless the rank one constraint is satisfied, i.e., $\text{rank}(\mathbf{Y}/\xi) = 1$. If not, we can perform the well-known Gaussian randomization procedure (GRP) to derive a feasible PS vector. Specifically, we carry out the eigenvalue decomposition of $\mathbf{Z} = \mathbf{Y}/\xi$, denoted as $\mathbf{Z} = \mathbf{U} \mathbf{\Sigma} \mathbf{U}^H$, and construct a random vector $\tilde{\mathbf{z}} = \mathbf{U} \mathbf{\Sigma}^{1/2} \mathbf{r}$, where $\mathbf{r} \in \mathbb{C}^{N+1}$ is a random vector following $\mathcal{CN}(\mathbf{0}, \mathbf{I})$. Then we can obtain a feasible PS vector as

$$\mathbf{v} = \left[\frac{\tilde{\mathbf{z}}(1)/\tilde{\mathbf{z}}(N+1)}{|\tilde{\mathbf{z}}(1)/\tilde{\mathbf{z}}(N+1)|}, \frac{\tilde{\mathbf{z}}(2)/\tilde{\mathbf{z}}(N+1)}{|\tilde{\mathbf{z}}(2)/\tilde{\mathbf{z}}(N+1)|}, \dots, \frac{\tilde{\mathbf{z}}(N)/\tilde{\mathbf{z}}(N+1)}{|\tilde{\mathbf{z}}(N)/\tilde{\mathbf{z}}(N+1)|} \right]. \quad (16)$$

By this means, \mathbf{v} is determined as the one which attains the maximum objective value of (P2) among a set of randomly generated PS vectors via GRP.

D. Lower-Complexity Algorithm

In the last subsection, we have proposed a CCT-based algorithm to characterize the secrecy rate region in the IRS-assisted PHY-SI. However, in this algorithm, we need to solve an SDP with the path-following approach at every point in the linear search, thus incurring high computational complexity. In this subsection, we propose a WSCM-based algorithm as a suboptimal alternative but with lower computational complexity. Specifically, we first derive an optimal covariance matrix \mathbf{Z}_m by solving (P3) for maximizing the multicast rate. Then we derive an optimal covariance matrix \mathbf{Z}_c for maximizing the secrecy rate, which can be obtained by solving the following SDP and setting $\mathbf{Z}_c = \mathbf{Y}_c/\xi_c$,

$$\begin{aligned}
 (\text{P5}) \quad & \{\mathbf{Y}_c, \xi_c\} = \arg \max_{\mathbf{Y}, \xi} \text{Tr}[\mathbf{Y}(\frac{\sigma_1^2 \sigma_2^2}{N+1} \mathbf{I} + \sigma_2^2 P \mathbf{T}_1)] \\
 \text{s.t.} \quad & \text{Tr}[\mathbf{Y}(\frac{\sigma_1^2 \sigma_2^2}{N+1} \mathbf{I} + \sigma_1^2 P \mathbf{T}_2)] = 1, \\
 & \text{Tr}(\mathbf{Y} \mathbf{E}_i) = \xi, \quad i = 1, 2, \dots, N+1, \\
 & \mathbf{Y} \succeq \mathbf{0}, \quad \xi > 0.
 \end{aligned} \tag{17}$$

The main idea is still by using the CCT. The details of deriving (P5) are thus omitted for brevity. By introducing a weight $\lambda \in [0, 1]$, we can construct a new covariance matrix, i.e.,

$$\mathbf{Z}(\lambda) = \lambda \mathbf{Z}_c + (1 - \lambda) \mathbf{Z}_m. \tag{18}$$

Next, we perform the GRP given in (16) to extract a PS vector $\mathbf{v}(\lambda)$ from $\mathbf{Z}(\lambda)$. By varying the weight λ within $[0, 1]$, we can obtain a set of $\mathbf{v}(\lambda)$ and then find the optimal one which leads to the maximum secrecy rate. Specifically, for each λ , we need to obtain its corresponding secrecy rate $R(\lambda)$ for comparison by optimizing the power allocation factor, i.e.,

$$(\text{P6}) \quad R(\lambda) = \max_{\alpha} \left[\log \frac{\sigma_1^2 \sigma_2^2 + \sigma_2^2 \alpha |\mathbf{m}_1^H \text{diag}[\mathbf{v}(\lambda)^*] \mathbf{g} + h_1|^2}{\sigma_1^2 \sigma_2^2 + \sigma_1^2 \alpha |\mathbf{m}_2^H \text{diag}[\mathbf{v}(\lambda)^*] \mathbf{g} + h_2|^2} \right]^+ \tag{19a}$$

$$\text{s.t.,} \quad \log \left(1 + \frac{(P - \alpha) |\mathbf{m}_2^H \text{diag}[\mathbf{v}(\lambda)^*] \mathbf{g} + h_2|^2}{\sigma_2^2 + \alpha |\mathbf{m}_2^H \text{diag}[\mathbf{v}(\lambda)^*] \mathbf{g} + h_2|^2} \right) \geq r_m, \tag{19b}$$

$$\alpha \geq 0, \quad P - \alpha \geq 0, \quad \lambda \geq 0, \quad 1 - \lambda \geq 0. \tag{19c}$$

where the QoMS constraint for user 1 is discarded due to (10). It is easy to find that the optimal solution to (P6), denoted as α_{opt} , can be derived in closed form. To be specific, since the objective function in (19a) monotonically increases with α given the condition (10), α_{opt} should be the largest one within $[0, P]$ that meets constraint (19b). In fact, (19b) can be rewritten as

$$(P - \alpha 2^{r_m}) |\mathbf{m}_2^H \text{diag}[\mathbf{v}(\lambda)^*] \mathbf{g} + h_2|^2 - (2^{r_m} - 1) \sigma_2^2 \geq 0. \tag{20}$$

It is easy to observe that the left hand side of (20) monotonically decreases with α . As a result, the optimal allocated power α_{opt} for transmitting the confidential message is given by

$$\alpha_{\text{opt}} = \left[\min \left\{ P, \frac{P |\mathbf{m}_2^H \text{diag}[\mathbf{v}(\lambda)^*] \mathbf{g} + h_2|^2 - (2^{r_m} - 1) \sigma_2^2}{2^{r_m} |\mathbf{m}_2^H \text{diag}[\mathbf{v}(\lambda)^*] \mathbf{g} + h_2|^2} \right\} \right]^+. \quad (21)$$

It is noted from (21) that the optimal transmit power allocated to the confidential message depends critically on the IRS passive beamforming \mathbf{v} . More detailed analysis on its impact will be presented in Section V. By substituting (21) into (P6), we can find the optimal weight λ_{opt} via the one dimensional search over λ within $[0, 1]$ and the corresponding PS design, i.e., $\mathbf{v}(\lambda_{\text{opt}})$, as well as the corresponding power allocation factors α_{opt} and $\beta_{\text{opt}} = P - \alpha_{\text{opt}}$.

IV. GENERAL MULTI-USER SYSTEM

In previous sections, we only discuss the proposed solution to (P1) in the case of $K = 2$. In this section, we consider the general but more challenging multi-user system with $K > 2$ and also analyze the performance gap to the globally optimal solutions.

A. CCT-based Algorithm for the Multi-User Case

Similarly as before, we fix the variable R_m as a constant r_m and the secrecy rate region maximization problem reduces to the maximization of R_c , i.e.,

$$(P7) : \bar{R}_c(r_m) = \max_{\alpha, \beta, \mathbf{v}} \min_{k \in \mathcal{E}} \left[\log \frac{\sigma_1^2 \sigma_k^2 + \sigma_k^2 \alpha |\mathbf{m}_1^H \text{diag}(\mathbf{v}^*) \mathbf{g} + h_1|^2}{\sigma_1^2 \sigma_k^2 + \sigma_k^2 \alpha |\mathbf{m}_k^H \text{diag}(\mathbf{v}^*) \mathbf{g} + h_k|^2} \right]^+ \quad (22a)$$

$$\text{s.t. } \log \left(1 + \frac{\beta |\mathbf{m}_k^H \text{diag}(\mathbf{v}^*) \mathbf{g} + h_k|^2}{\sigma_k^2 + \alpha |\mathbf{m}_k^H \text{diag}(\mathbf{v}^*) \mathbf{g} + h_k|^2} \right) \geq r_m, \quad \forall k \in \mathcal{K}, \quad (22b)$$

$$\alpha + \beta \leq P, \quad \alpha \geq 0, \quad \beta \geq 0, \quad |\mathbf{v}(i)| = 1, \quad i = 1, 2, \dots, N. \quad (22c)$$

By varying the parameter r_m within $[0, r_m^{\text{up}}]$, we can find all the boundary points in (P7) and the upper-bound desired multicast rate r_m^{up} in the QoMS constraint can be obtained by solving the following extended SDR from ($\hat{P}3$), i.e.,

$$(P8) : r_m^{\text{up}} = \max_{\mathbf{Z}, \tau} \tau \quad (23)$$

$$\text{s.t. } \text{Tr} \left(\frac{P}{\sigma_k^2} \mathbf{Z} \mathbf{T}_k \right) \geq 2^\tau - 1, \quad \forall k \in \mathcal{K},$$

$$\text{Tr}(\mathbf{Z} \mathbf{E}_i) = 1, \quad i = 1, \dots, N+1, \quad \mathbf{Z} \succeq \mathbf{0}.$$

In the general multi-user case, the necessary condition for $\bar{R}_c(0) > 0$ can be expressed as

$$\frac{|\mathbf{m}_1^H \text{diag}(\mathbf{v}^*) \mathbf{g} + h_1|^2}{\sigma_1^2} > \max_k \frac{|\mathbf{m}_k^H \text{diag}(\mathbf{v}^*) \mathbf{g} + h_k|^2}{\sigma_k^2}. \quad (24)$$

In this case, the QoMS constraint for user 1 in (22b) can be discarded and solving (P7) is equivalent to solving (P9),

$$\begin{aligned}
(\text{P9}) : \quad & 2^{\bar{R}_c(r_m)} = \max_{\alpha, \mathbf{Z}} \min_{k \in \mathcal{E}} \frac{\text{Tr}[\mathbf{Z}(\frac{\sigma_1^2 \sigma_k^2}{N+1} \mathbf{I} + \sigma_k^2 \alpha \mathbf{T}_1)]}{\text{Tr}[\mathbf{Z}(\frac{\sigma_1^2 \sigma_k^2}{N+1} \mathbf{I} + \sigma_1^2 \alpha \mathbf{T}_k)]} \\
\text{s.t.} \quad & \frac{\text{Tr}[(P - \alpha) \mathbf{Z} \mathbf{T}_k]}{\text{Tr}[\mathbf{Z}(\frac{\sigma_k^2}{N+1} \mathbf{I} + \alpha \mathbf{T}_k)]} \geq 2^{r_m} - 1, \quad k \in \mathcal{E}, \\
& \text{Tr}(\mathbf{Z} \mathbf{E}_i) = 1, \quad i = 1, 2, \dots, N+1, \\
& \text{rank}(\mathbf{Z}) = 1, \quad \mathbf{Z} \succeq \mathbf{0}, \quad \alpha \geq 0, \quad P - \alpha \geq 0.
\end{aligned} \tag{25}$$

Due to the minimum operator in the objective function of (P9), we need to further rewrite it as a more tractable form before applying the CCT, i.e.,

$$\min_{k \in \mathcal{E}} \frac{\text{Tr}[\mathbf{Z}(\frac{\sigma_1^2 \sigma_k^2}{N+1} \mathbf{I} + \sigma_k^2 \alpha \mathbf{T}_1)]}{\text{Tr}[\mathbf{Z}(\frac{\sigma_1^2 \sigma_k^2}{N+1} \mathbf{I} + \sigma_1^2 \alpha \mathbf{T}_k)]} = \min_{k \in \mathcal{E}} \frac{\text{Tr}[\frac{\mathbf{Y}}{\xi}(\frac{\sigma_1^2 \sigma_k^2}{N+1} \mathbf{I} + \sigma_k^2 \alpha \mathbf{T}_1)]}{\text{Tr}[\frac{\mathbf{Y}}{\xi}(\frac{\sigma_1^2 \sigma_k^2}{N+1} \mathbf{I} + \sigma_1^2 \alpha \mathbf{T}_k)]} = \frac{\text{Tr}[\mathbf{Y}(\frac{\sigma_1^2}{N+1} \mathbf{I} + \alpha \mathbf{T}_1)]}{\max_{k \in \mathcal{E}} \text{Tr}[\mathbf{Y}(\frac{\sigma_1^2}{N+1} \mathbf{I} + \frac{\sigma_k^2}{\sigma_1^2} \alpha \mathbf{T}_k)]}. \tag{26}$$

Notice that by properly selecting an auxiliary variable ξ , the denominator of the last equation in (26) can be any positive real number. Thus, we can introduce this auxiliary variable ξ along with an additional constraint, i.e., $\max_{k \in \mathcal{E}} \text{Tr}[\mathbf{Y}(\frac{\sigma_1^2}{N+1} \mathbf{I} + \frac{\sigma_k^2}{\sigma_1^2} \alpha \mathbf{T}_k)] = 1$, without loss of optimality. Then, (P9) can be rewritten as an SDR, which is given by

$$(\text{P10}) : \quad C(r_m) = \max_{\alpha, \mathbf{Y}, \xi} \text{Tr}[\mathbf{Y}(\frac{\sigma_1^2}{N+1} \mathbf{I} + \alpha \mathbf{T}_1)] \tag{27a}$$

$$\text{s.t.} \quad \text{Tr}[\mathbf{Y}(\frac{\sigma_1^2}{N+1} \mathbf{I} + \frac{\sigma_k^2}{\sigma_1^2} \alpha \mathbf{T}_k)] \leq 1, \quad \forall k \in \mathcal{E}, \tag{27b}$$

$$\text{Tr} \left\{ \mathbf{Y} \left[(P - \alpha 2^{r_m}) \mathbf{T}_k - \frac{(2^{r_m} - 1) \sigma_k^2}{N+1} \mathbf{I} \right] \right\} \geq 0, \quad \forall k \in \mathcal{E}, \tag{27c}$$

$$\text{Tr}(\mathbf{Y} \mathbf{E}_i) = \xi, \quad i = 1, 2, \dots, N+1, \tag{27d}$$

$$\mathbf{Y} \succeq \mathbf{0}, \quad \alpha \geq 0, \quad P - \alpha \geq 0, \quad \xi > 0. \tag{27e}$$

It is easy to observe that (P10) is an SDP with any fixed α ; thus, its optimal solution can be derived by performing the following steps. Specifically, let $(\tilde{\alpha}, \tilde{\mathbf{Y}}, \tilde{\xi})$ be an optimal solution to (P10). We aim to find $\tilde{\alpha}$ by performing a uniform search over α in the following convex optimization problem,

$$\begin{aligned}
(\hat{\text{P10}}) : \quad & C(r_m, \alpha) = \max_{\mathbf{Y}, \xi} \text{Tr}[\mathbf{Y}(\frac{\sigma_1^2}{N+1} \mathbf{I} + \alpha \mathbf{T}_1)] \\
\text{s.t.} \quad & (27b), (27c), (27d), \quad \mathbf{Y} \succeq \mathbf{0}, \quad \xi > 0.
\end{aligned} \tag{28}$$

Obviously, when $\alpha = \tilde{\alpha}$, we can obtain $(\tilde{\mathbf{Y}}, \tilde{\xi})$. While $(\hat{\text{P10}})$ may not be tight, the GRP can be used to obtain a feasible \mathbf{v} from a higher-rank solution. The detailed steps of the generalized CCT-based approach are summarized in Algorithm 1, where T_α is the number of uniformly sampling points of α .

Algorithm 1 Generalized CCT-based Approach for Characterizing the secrecy rate region

Given: $P, \{\sigma_k^2\}_{k=1}^K, \mathbf{g}, \{h_k\}_{k=1}^K, \{\mathbf{m}_k^H\}_{k=1}^K, T_\alpha$.

- 1: **Initialization:** $\mathcal{K} \triangleq \{1, 2, \dots, K\}, \mathcal{E} \triangleq \mathcal{K}/\{1\}, \overline{R}_c(r_m) = 0$.
 - 2: Compute $\mathbf{T}_k = \begin{bmatrix} \text{diag}(\mathbf{m}_k^*)\mathbf{g}\mathbf{g}^H\text{diag}(\mathbf{m}_k) & \text{diag}(\mathbf{m}_k^*)\mathbf{g}h_k^* \\ h_k\mathbf{g}^H\text{diag}(\mathbf{m}_k) & h_k^*h_k \end{bmatrix}, k \in \mathcal{K}$.
 - 3: Find r_m^{up} by solving (P8).
 - 4: Vary r_m within $[0, r_m^{\text{up}}]$ and obtain $\overline{R}_c(r_m)$ through the following steps.
 - 5: **for** $t = 1 : T_\alpha$ **do**
 - 6: $\alpha_t = P(t - 1)/(T_\alpha - 1)$.
 - 7: Find \mathbf{Y} and ξ by solving $(\hat{\text{P10}})$ with $\alpha = \alpha_t$.
 - 8: **if** $(\hat{\text{P10}})$ is feasible **then**
 - 9: Perform the GRP and obtain a feasible PS vector \mathbf{v}_t by (16).
 - 10: Compute $R_c(r_m, \alpha_t) = \min_{k \in \mathcal{E}} \left[\log \frac{\sigma_1^2 \sigma_k^2 + \sigma_k^2 \alpha_t |\mathbf{m}_1^H \text{diag}(\mathbf{v}_t^*) \mathbf{g} + h_1|^2}{\sigma_1^2 \sigma_k^2 + \sigma_1^2 \alpha_t |\mathbf{m}_k^H \text{diag}(\mathbf{v}_t^*) \mathbf{g} + h_k|^2} \right]^+$.
 - 11: **if** $R_c(r_m, \alpha_t) > \overline{R}_c(r_m)$ **then** $\overline{R}_c(r_m) = R_c(r_m, \alpha_t)$. **end if**
 - 12: **end if**
 - 13: **end for**
- Return:** $\overline{R}_c(r_m)$.
-

It is worth noting that the logarithm of $C(r_m, \tilde{\alpha})$ in $(\hat{\text{P10}})$ serves as an upper bound on the maximum achievable secrecy rate, which will be used as a benchmark in Section VI to evaluate the performance of our proposed algorithms. Given an arbitrary $\tilde{\alpha} \in [0, P]$, we find via simulations that the achievable secrecy rate can reach the upper bound in most cases, i.e., $R_c(r_m, \tilde{\alpha}) = \log[C(r_m, \tilde{\alpha})]$. In this case, $(\hat{\text{P10}})$ is tight and any boundary point of the secrecy rate region can be characterized as long as $R_c(r_m, \tilde{\alpha})$ is found. However, $\tilde{\alpha}$ may not be exactly found by the one-dimensional search with uniform and finite sampling in Algorithm 1. Besides, $R_c(r_m, \alpha)$ does not monotonically change with α since it is also affected by the optimal PS vector \mathbf{v} . Thus, it is challenging to characterize the relationship between the performance gap and the uniform search times in Algorithm 1. In the following Proposition 2, we first characterize

the relationship by assuming $(\hat{P}10)$ is tight.

Proposition 2. Assume that $(\hat{P}10)$ is tight, i.e., $R_c(r_m, \tilde{\alpha})$ is the globally optimal solution to (P7). T_α and $\bar{R}_c(r_m)$ are the number of sampling points and the obtained solution by Algorithm 1, respectively. Let $R_\Delta \triangleq R_c(r_m, \tilde{\alpha}) - \bar{R}_c(r_m)$ be the performance gap. Then, we have

$$R_\Delta \leq \log \left[1 + \frac{P(N+1)\text{Tr}(\mathbf{T}_1)}{\sigma_1^2(T_\alpha - 1)} \right]. \quad (29)$$

Proof. See Appendix B. □

Proposition 2 shows that if the solution obtained by steps 7-10 in Algorithm 1 is equal to the performance upper bound, i.e., $R_c(r_m, \alpha) = \log[C(r_m, \alpha)]$, the performance gap R_Δ decreases to zero when T_α is sufficiently large. Due to the difficulty in characterizing the rank profile of the solution to $(\hat{P}10)$ analytically, it is important to further characterize the relationship between R_Δ and T_α in the case that $(\hat{P}10)$ is not tight, i.e., $R_c(r_m, \alpha) \leq \log[C(r_m, \alpha)]$.

Corollary 1. Let $c = \arg \max_{t=1,2,\dots,T_\alpha} R_c(r_m, \alpha_t)$ be the index of the best sampling points in Algorithm 1, i.e., $R_c(r_m, \alpha_c) = \bar{R}_c(r_m)$. Then, we have

$$R_\Delta \leq \log \left[1 + \frac{P(N+1)\text{Tr}(\mathbf{T}_1)}{\sigma_1^2(T_\alpha - 1)} \right] + \Delta_c. \quad (30)$$

where $\Delta_c = \log[C(r_m, \alpha_c)] - R_c(r_m, \alpha_c)$ is the gap between the performance upper-bound and Algorithm 1. Without knowing Δ_c , it ensures the worst-case performance

$$R_\Delta \leq \log \left[\frac{4}{\pi} + \frac{4P(N+1)\text{Tr}(\mathbf{T}_1)}{\pi\sigma_1^2(T_\alpha - 1)} \right]. \quad (31)$$

Proof. See Appendix C. □

To bound the performance gap $R_\Delta = R_c(r_m, \tilde{\alpha}) - R_c(r_m, \alpha_c)$, although it seems that the tightness levels of $(\hat{P}10)$ in terms of $\alpha = \tilde{\alpha}$ and $\alpha = \alpha_c$ are both needed, (30) suggests that it suffices to know the latter, i.e., the gap between $R_c(r_m, \alpha_c)$ and $\log[C(r_m, \alpha_c)]$. When T_α is sufficiently large, R_Δ must be less than Δ_c . Consequently, after obtaining a solution from Algorithm 1, one can obtain the index c and check Δ_c by calculating $\log[C(r_m, \alpha_c)]$, thereby evaluating the quality of this solution. Meanwhile, (31) guarantees that R_Δ must be no more than $\log(4/\pi)$ even without any knowledge of Δ_c .

B. WSCM-based Algorithm for the Multi-User Case

In this subsection, we extend the WSCM-based algorithm to the general multi-user system. Similarly, we first derive the matrix \mathbf{Z}_m by (P8) for maximizing the multicast rate. Then we derive the matrix \mathbf{Z}_c for maximizing the secrecy rate by solving the following SDP and setting $\mathbf{Z}_c = \mathbf{Y}_c/\xi_c$, i.e.,

$$\begin{aligned}
 \text{(P11)} : \quad & \{\mathbf{Y}_c, \xi_c\} = \arg \max_{\mathbf{Y}, \xi} \text{Tr}[\mathbf{Y}(\frac{\sigma_1^2}{N+1}\mathbf{I} + P\mathbf{T}_1)] \\
 & \text{s.t. } \text{Tr}[\mathbf{Y}(\frac{\sigma_1^2}{N+1}\mathbf{I} + \frac{\sigma_1^2}{\sigma_k^2}P\mathbf{T}_k)] \leq 1, \quad \forall k \in \mathcal{E}, \\
 & \text{Tr}(\mathbf{Y}\mathbf{E}_i) = \xi, \quad i = 1, 2, \dots, N+1, \\
 & \mathbf{Y} \succeq \mathbf{0}, \quad \alpha \geq 0, \quad P - \alpha \geq 0, \quad \xi > 0.
 \end{aligned} \tag{32}$$

Next, we construct the WSCM by using (18). By varying the weight λ within $[0, 1]$, we need to find the optimal one that leads to the maximum secrecy rate by solving

$$\text{(P12)} \quad R(\lambda) = \max_{\alpha} \min_{k \in \mathcal{E}} \left[\log \frac{\sigma_1^2 \sigma_k^2 + \sigma_k^2 \alpha |\mathbf{m}_1^H \text{diag}[\mathbf{v}(\lambda)^*] \mathbf{g} + h_1|^2}{\sigma_1^2 \sigma_k^2 + \sigma_1^2 \alpha |\mathbf{m}_k^H \text{diag}[\mathbf{v}(\lambda)^*] \mathbf{g} + h_k|^2} \right]^+ \tag{33a}$$

$$\text{s.t.}, \quad \log \left(1 + \frac{(P - \alpha) |\mathbf{m}_k^H \text{diag}[\mathbf{v}(\lambda)^*] \mathbf{g} + h_k|^2}{\sigma_k^2 + \alpha |\mathbf{m}_k^H \text{diag}[\mathbf{v}(\lambda)^*] \mathbf{g} + h_k|^2} \right) \geq r_m, \quad \forall k \in \mathcal{E}. \tag{33b}$$

$$\alpha \geq 0, \quad P - \alpha \geq 0, \quad \lambda \geq 0, \quad 1 - \lambda \geq 0. \tag{33c}$$

Let $\tau = \arg \min_k |\mathbf{m}_k^H \text{diag}[\mathbf{v}(\lambda)^*] \mathbf{g} + h_k|^2 / \sigma_k^2$. Due to the monotonicity of $(P - \alpha)x / (1 + \alpha x)$ w.r.t. x (where $x \in \{|\mathbf{m}_k^H \text{diag}[\mathbf{v}(\lambda)^*] \mathbf{g} + h_k|^2 / \sigma_k^2\}_{k=1}^K$), we only need to consider the QoMS constraint of user τ in (33b). Since the objective function of (33a) increases with α , the optimal α_{opt} should be the largest α that satisfies the QoMS constraint for user τ , which is given by

$$\alpha_{\text{opt}} = \left[\min \left\{ P, \frac{P |\mathbf{m}_\tau^H \text{diag}[\mathbf{v}(\lambda)^*] \mathbf{g} + h_\tau|^2 - (2^{r_m} - 1) \sigma_\tau^2}{2^{r_m} |\mathbf{m}_\tau^H \text{diag}[\mathbf{v}(\lambda)^*] \mathbf{g} + h_\tau|^2} \right\} \right]^+. \tag{34}$$

By substituting (34) into (P12), we can find λ_{opt} via a one dimensional search within $[0, 1]$. All detailed steps are summarized in Algorithm 2, where T_λ is the number of uniformly sampling points of λ .

C. Complexity Analysis

In this subsection, we give the computational complexity of the proposed algorithms in finding a boundary point of the secrecy rate region. The complexity of both the CCT-based and WSCM-based algorithms depend on the line search precision. We assume that a standard

Algorithm 2 WSCM-based Algorithm for Transmit Design with QoMS.

Given: r_m , P , $\{\sigma_k^2\}_{k=1}^K$, \mathbf{g} , $\{h_k\}_{k=1}^K$, $\{\mathbf{m}_k^H\}_{k=1}^K$.

- 1: **Initialization:** $\mathcal{K} \triangleq \{1, 2, \dots, K\}$, $\mathcal{E} \triangleq \mathcal{K}/\{1\}$, $\bar{R}_c(r_m) = 0$.
 - 2: Compute $\mathbf{T}_k = \begin{bmatrix} \text{diag}(\mathbf{m}_k^*) \mathbf{g} \mathbf{g}^H \text{diag}(\mathbf{m}_k) & \text{diag}(\mathbf{m}_k^*) \mathbf{g} h_k^* \\ h_k \mathbf{g}^H \text{diag}(\mathbf{m}_k) & h_k^* h_k \end{bmatrix}$, $k \in \mathcal{K}$.
 - 3: Find \mathbf{Z}_m by solving (P8).
 - 4: Find \mathbf{Z}_c by solving (P11).
 - 5: **for** $t = 1 : T_\lambda$ **do**
 - 6: $\lambda_t = (t - 1)/(T_\lambda - 1)$.
 - 7: $\mathbf{Z}(\lambda_t) = \lambda_t \mathbf{Z}_c + (1 - \lambda_t) \mathbf{Z}_m$.
 - 8: Perform the GRP and obtain a feasible PS vector \mathbf{v}_t by (16).
 - 9: $\tau = \arg \min_k |\mathbf{m}_k^H \text{diag}[\mathbf{v}(\lambda_t)^*] \mathbf{g} + h_k|^2 / \sigma_k^2$,
 - 10: $\rho_t = |\mathbf{m}_\tau^H \text{diag}[\mathbf{v}(\lambda_t)^*] \mathbf{g} + h_\tau|^2 / \sigma_\tau^2$.
 - 11: $\alpha_t = \left[\min \left\{ P, \frac{P}{2^{r_m}} - \frac{1}{\rho_t} + \frac{1}{2^{r_m} \rho_t} \right\} \right]^+$.
 - 12: Compute $R_c(t) = \min_{k \in \mathcal{E}} \left[\log \frac{\sigma_1^2 \sigma_k^2 + \sigma_k^2 \alpha_t |\mathbf{m}_1^H \text{diag}(\mathbf{v}_t^*) \mathbf{g} + h_1|^2}{\sigma_1^2 \sigma_k^2 + \sigma_1^2 \alpha_t |\mathbf{m}_k^H \text{diag}(\mathbf{v}_t^*) \mathbf{g} + h_k|^2} \right]^+$.
 - 13: **if** $R_c(t) > \bar{R}_c(r_m)$ **then** $\bar{R}_c(r_m) = R_c(t)$. **end if**
 - 14: **end if**
 - 15: **end for**
- Return:** $\bar{R}_c(r_m)$.
-

interior-point method is used to solve the SDPs required in the proposed algorithms and T_g times of randomizations are used in GRP to obtain a feasible solution. We use A_n^m to represent the computational complexity of the m th part in Algorithm n . In Algorithm 1, (P8) is subjected to one linear matrix inequality (LMI) constraint of size $N + 1$, $K - 1$ LMI constraints of size 1, and $N + 1$ linear matrix equality (LME) constraints of size 1. The computational cost incurred to find an ϵ -optimal solution to $(\hat{\text{P8}})$ is on the order of $\ln(1/\epsilon) \sqrt{\psi} \zeta$, where $\psi = 2N + K + 1$ is the geometric complexity, $\zeta = n[(N + 1)^3 + K + N] + n^2[(N + 1)^2 + K + N] + n^3$ is the cost per iteration, and $n = \mathcal{O}[(N + 1)^2 + 1]$. Hence, the complexity of (P8) is given by (suppressing $\ln(1/\epsilon)$)

$$A_1^1 = \sqrt{2N + K + 1} [n((N + 1)^3 + K + N) + n^2((N + 1)^2 + K + N) + n^3]. \quad (35)$$

(P10) is subjected to one LMI constraint of size $N + 1$, $2K - 1$ LMI constraints of size 1, and $N + 1$ LME constraints of size 1. Thus, the complexity of (P10) is given by

$$A_1^2 = \sqrt{2N + 2K + 1} [n((N + 1)^3 + 2K + N) + n^2((N + 1)^2 + 2K + N) + n^3]. \quad (36)$$

The complexity of GRP is on the order of $G = (N + 1)^3 + 8T_g(N + 1)^2$. As a result, the complexity of Algorithm 1 for finding a boundary point $\bar{R}_c(r_m)$ is on the order of

$$A_1 = A_1^1 + T_\alpha(A_1^2 + G). \quad (37)$$

In Algorithm 2, the complexity of (P8) is given by (61) and we have $A_2^1 = A_1^1$. (P11) is subjected to one LMI constraint of size $N + 1$, $K + 2$ LMI constraints of size 1, and $N + 1$ LME constraints of size 1. Thus, the complexity of (P11) is given by

$$A_2^2 = \sqrt{2N + K + 4} [n((N + 1)^3 + K + N + 3) + n^2((N + 1)^2 + K + N + 3) + n^3]. \quad (38)$$

Consequently, the complexity of Algorithm 2 for finding a boundary point is on the order of

$$A_2 = A_2^1 + A_2^2 + T_\lambda G. \quad (39)$$

We find via simulation that it only takes $T_\lambda < \mathcal{O}(N^2)$ search times to achieve a comparable performance to the upper bound. Accordingly, the overall complexity of Algorithm 1 and Algorithm 2 are given by $\mathcal{O}(T_\alpha N^{5.5})$ and $\mathcal{O}(N^{5.5})$, respectively.

V. THEORETICAL ANALYSIS

In this section, we analyze the impact of IRS passive beamforming or PSs on the performance of PHY-SI. Comparing to the traditional system without IRS, we aim to figure out how the IRS affects the secrecy rate region or its underlying mechanism. For simplicity, we take the two-user case as an example while the insights revealed can be extended to the general multi-user case similarly. The secrecy rate achieved in the traditional system is given by

$$R_c^{\text{non}} = \left[\log \left(\frac{1 + \alpha \frac{|h_1|^2}{\sigma_1^2}}{1 + \alpha \frac{|h_2|^2}{\sigma_2^2}} \right) \right]^+. \quad (40)$$

We assume non-zero R_c^{non} is achievable; thus, we have

$$\frac{|h_1|^2}{\sigma_1^2} > \frac{|h_2|^2}{\sigma_2^2}. \quad (41)$$

With the assistance of IRS, the secrecy rate achieved in the IRS-assisted system is given by

$$R_c^{\text{IRS}} = \left[\log \left(\frac{1 + \alpha \frac{|\mathbf{m}_1^H \text{diag}(\mathbf{v}^*) \mathbf{g} + h_1|^2}{\sigma_1^2}}{1 + \alpha \frac{|\mathbf{m}_2^H \text{diag}(\mathbf{v}^*) \mathbf{g} + h_2|^2}{\sigma_2^2}} \right) \right]^+. \quad (42)$$

Considering the monotonicity of the logarithm function, we only focus on the term inside it. Define the following function

$$r(\alpha) = \frac{1 + \alpha \frac{|h_1|^2}{\sigma_1^2}}{1 + \alpha \frac{|h_2|^2}{\sigma_2^2}}. \quad (43)$$

It is easy to verify that $r(\alpha)$ increases with α under the condition (41), which implies that *a larger α yields better secrecy-rate performance*. Given a desired multicast rate r_m , the optimal α (see (21)) can be rewritten as

$$\alpha^{\text{opt}} = \frac{Px - c_1}{c_2 x}, \quad (44)$$

where $c_1 = (2^{r_m} - 1)\sigma_2^2$, $c_2 = 2^{r_m}$, and

$$x = \begin{cases} |h_2|^2, & \text{without IRS} \\ |\mathbf{m}_2^H \text{diag}(\mathbf{v}^*)\mathbf{g} + h_2|^2, & \text{with IRS} \end{cases}. \quad (45)$$

By checking the first-order derivative, it can be verified that α^{opt} monotonically increases with x . Thus, compared to the traditional no-IRS system, if $|\mathbf{m}_2^H \text{diag}[\mathbf{v}(\lambda)^*]\mathbf{g} + h_2|^2 > |h_2|^2$, the power α^{opt} is larger in the IRS-assisted system. *Hence, the larger channel gain of user 2 brought by the IRS, the larger portion of transmit power α allocated to the confidential message.*

Next, we discuss how the variation of the channels affects the secrecy rate in the IRS-assisted system. Assume that in both systems, we allocate an equal transmit power α to the confidential message. Let E_1 and E_2 represent the channel enhancement brought by the IRS for user 1 and user 2, respectively, i.e.,

$$E_k = \frac{1 + \alpha \frac{|\mathbf{m}_k^H \text{diag}(\mathbf{v}^*)\mathbf{g} + h_k|^2}{\sigma_k^2}}{1 + \alpha \frac{|h_k|^2}{\sigma_k^2}}, \quad k \in \{1, 2\}. \quad (46)$$

As such, the secrecy rates R_c^{non} and R_c^{IRS} (defined in (40) and (42), respectively) follow

$$2^{R_c^{\text{IRS}}} = \frac{E_1}{E_2} \cdot 2^{R_c^{\text{non}}}. \quad (47)$$

Let $\eta = \frac{E_1}{E_2}$ represent the resulting secrecy-rate enhancement with fixed α . It is obvious that if $\eta > 1$, the secrecy rate achieved is larger in the IRS-assisted system. Moreover, a larger η yields a larger security performance gain.

Based on the above discussions, it is noted that the maximum achievable secrecy rate in IRS-assisted system is proportional to α and η . *Thus, the security performance in the IRS-assisted system would outperform that in the traditional system if both α and η are enlarged by IRS.* To enlarge α under a given QoMS constraint, one can leverage IRS to enhance the channel gain

of user 2. However, while IRS improves the channel gain of user 2, it also changes the channel gain of user 1. If the enhancement brought to user 2 is larger than that to user 1, i.e., $E_2 > E_1$, the secrecy-rate performance, in turn, will be impaired. As a result, there exists an interesting trade-off between enhancing the channel of user 1 and that of user 2.

Proposition 3. *For any given IRS with PS vector \mathbf{v} , compared to the traditional system, the secrecy-rate performance of the IRS-assisted system is higher if*

$$\begin{aligned} |\mathbf{m}_2^H \text{diag}(\mathbf{v}^*)\mathbf{g} + h_2| &> |h_2| \quad \text{and} \\ |h_2| \cdot |\mathbf{m}_1^H \text{diag}(\mathbf{v}^*)\mathbf{g} + h_1| &> |h_1| \cdot |\mathbf{m}_2^H \text{diag}(\mathbf{v}^*)\mathbf{g} + h_2|. \end{aligned} \quad (48)$$

On the contrary, IRS must impair the secrecy-rate performance if

$$\begin{aligned} |\mathbf{m}_2^H \text{diag}(\mathbf{v}^*)\mathbf{g} + h_2| &< |h_2| \quad \text{and} \\ |h_2| \cdot |\mathbf{m}_1^H \text{diag}(\mathbf{v}^*)\mathbf{g} + h_1| &< |h_1| \cdot |\mathbf{m}_2^H \text{diag}(\mathbf{v}^*)\mathbf{g} + h_2|. \end{aligned} \quad (49)$$

Proof. We point out that (48) ensures that both α and η are enlarged by IRS. The first inequality is easy to prove due to the monotonicity of (44). Next, we prove that the second inequality is a sufficient condition to increase η . Let $m_k = |\mathbf{m}_k^H \text{diag}(\mathbf{v}^*)\mathbf{g} + h_k|^2 / |h_k|^2$, $k \in \{1, 2\}$. Then, the second inequality is equivalent to $m_1 > m_2$. Notice that the first inequality implies that $m_2 > 1$, then we have the following relation

$$E_2 = \frac{1 + m_2 \cdot \alpha \frac{|h_2|^2}{\sigma_2^2}}{1 + \alpha \frac{|h_2|^2}{\sigma_2^2}} < \frac{1 + m_2 \cdot \alpha \frac{|h_1|^2}{\sigma_1^2}}{1 + \alpha \frac{|h_1|^2}{\sigma_1^2}} < \frac{1 + m_1 \cdot \alpha \frac{|h_1|^2}{\sigma_1^2}}{1 + \alpha \frac{|h_1|^2}{\sigma_1^2}} = E_1, \quad (50)$$

where the first inequality is due to (65) and that the function $\frac{1+m_1 \cdot \alpha x}{1+\alpha x}$ increases with x when $m_2 > 1$. Hence, the second inequality implies that η is enlarged by IRS, i.e., $\eta > 1$. On the contrary, it is easy to verify that (49) implies that both α and η are diminished, which completes the proof. \square

Given an IRS PS vector \mathbf{v} , Proposition 3 provides two sufficient conditions to easily evaluate the effects of IRS PS design in terms of secrecy-rate performance. In particular, it reveals that *not all* IRS PS designs can improve the secrecy-rate performance.

VI. NUMERICAL RESULTS

In this section, numerical results are provided to demonstrate the performance of the considered IRS-assisted PHY-SI by our proposed algorithms compared to that without IRS. Assuming a three-dimensional (3D) Cartesian coordinate system, we consider a uniform planar array (UPA)

at the IRS and assume all terminals are located in the x - z plane without loss of generality. The large-scale path loss is given by

$$L(d) = L_0 + 10 \log \left(\frac{d}{D_0} \right)^a. \quad (51)$$

where L_0 is the path-loss at the reference distance $D_0 = 1$ m, and a is the path-loss exponent. Due to the scattered obstacles, we set the path-loss exponent between the AP and users as $a_{\text{BU}} = 3.75$. By properly choosing the location of the IRS, we assume that all IRS-involved links experience approximately free-space path loss. As such, the path-loss exponents of IRS involved links are much smaller than that of AP-user link and is set as $a_{\text{IRS}} = 2.2$. The small-scale fading is assumed to be Rician fading, i.e.,

$$\mathbf{H} = \sqrt{\frac{\kappa}{1+\kappa}} \mathbf{a}_r(\phi_r, \omega_r) \mathbf{a}_t(\phi_t, \omega_t)^H + \sqrt{\frac{1}{1+\kappa}} \mathbf{H}^{\text{NLoS}}, \quad (52)$$

where κ is the Rician factor and the variables ϕ_t (resp. ω_t) and $\phi_r \in [0, 2\pi)$ (resp. ω_r) are the azimuth (resp. elevation) angles of departure and arrival for the line-of-sight (LoS) component, respectively. In the case of a UPA in the yz -plane with $N_t = N_y \times N_z$ elements, the array response vector can be expressed as,

$$\mathbf{a}(\phi, \omega) = \frac{1}{\sqrt{N_t}} [1, \dots, e^{jkd_a(n_y \sin \phi \sin \omega + n_z \cos \omega)}, \dots, e^{jkd_a(N_y \sin \phi \sin \omega + N_z \cos \omega)}]^T, \quad (53)$$

where $1 < n_y < N_y$, $1 < n_z < N_z$, $k = 2\pi/\lambda$, λ is the wavelength, and d_a is the element spacing. In particular, we have $\mathbf{a}_t = 1$ for AP-IRS link, $\mathbf{a}_r = 1$ for IRS-user links, and $\mathbf{a}_t = \mathbf{a}_r = 1$ for AP-user links. \mathbf{H}^{NLoS} is assumed to be Rayleigh fading channel and its entries are randomly generated following complex Gaussian distribution with zero mean and unit variance. Unless otherwise specified, in the simulation, we set $N = 10$, $P = 1\text{W}$, $T_\alpha = T_\lambda = 80$, $L_0 = 30\text{dB}$, $d_a = \lambda/2$, $\kappa = 10$, and $\{\sigma_k^2\}_{k=1}^K = -80\text{dBm}$.

A. Two-User Case, $K = 2$

First, we consider the two-user scenario. As shown in Fig. 2, AP, IRS, and user 2 are located at $(0, 0, 30)$, $(30, 0, 30)$, and $(30, 0, -10)$ respectively. User 1 is located at $(0, 0, d_1)$ and we will study the effect of d_1 on the performance of PHY-SI later. The center of the IRS is directly pointing to the origin and the parameters of all channels involved are summarized in Table I. We compare our proposed CCT-based and WSCM-based algorithms with the following benchmark schemes:

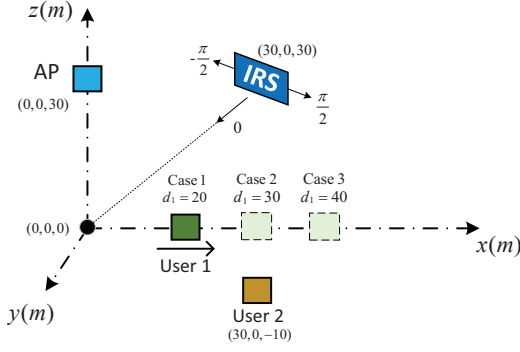


Fig. 2. Simulation setup of the two-user scenario.

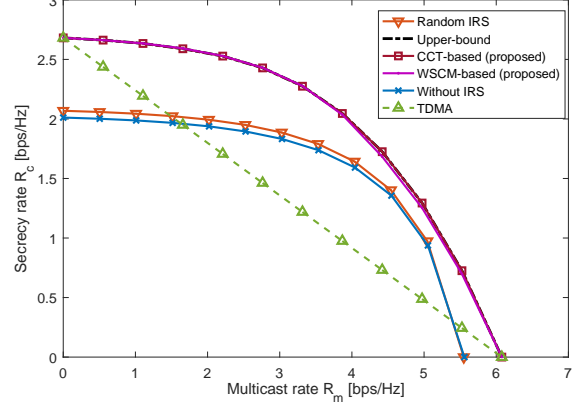


Fig. 3. Secrecy rate regions under different schemes in a two-user scenario.

TABLE I
SIMULATION PARAMETERS OF CHANNELS

Link	AP-IRS	AP-user 1	AP-user 2	IRS-user 1	IRS-user 2
Distance (m)	30	$\sqrt{30^2 + d_1^2}$	50	$\sqrt{30^2 + (30 - d_1)^2}$	40
AoA	$\phi_r^{AI} = -\frac{\pi}{4}, \omega_r^{AI} = \frac{\pi}{2}$	—	—	—	—
AoD	—	—	—	$\phi_t^{IU_1} = \arctan\left(\frac{30}{30-d_1}\right) - \frac{\pi}{4}$ $\omega_t^{IU_1} = \pi/2$	$\phi_t^{IU_2} = \pi/4$ $\omega_t^{IU_2} = \pi/2$
LoS component	$\mathbf{a}_r(\phi_r^{AI}, \omega_r^{AI})$	1	1	$\mathbf{a}_t(\phi_t^{IU_1}, \omega_t^{IU_1})^H$	$\mathbf{a}_t(\phi_t^{IU_2}, \omega_t^{IU_2})^H$

- **Random IRS:** The PS vector \mathbf{v} is randomly generated, with $|\mathbf{v}(i)| = 1$, $i = 1, 2, \dots, N$. Then, the maximum secrecy rate under the QoMS is obtained by using the optimal power allocation given in (44).
- **Upper-bound:** Given each r_m , we find α_c via the CCT-based algorithm and obtain the upper bound $\log[C(r_m, \alpha_c)]$ by solving $(\hat{P}10)$.
- **Time division multiple address (TDMA):** The multicast message and confidential message are assigned into orthogonal time slots.
- **Without IRS:** In this scheme, we assume that there is no IRS in the system and the optimal power allocation is given in (44).

Fig. 3 illustrates the secrecy rate regions achieved by our considered six schemes with $d_1 = 20$. First of all, let us focus on the performance of our proposed CCT-based and WSCM-based algorithms. It is observed that the CCT-based algorithm can achieve comparable performance to the upper bound, which validates its efficacy. Comparing the WSCM-based algorithm to the

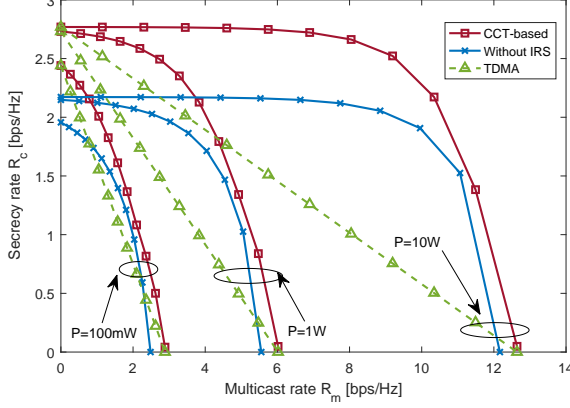


Fig. 4. Secrecy rate regions versus the transmit power.

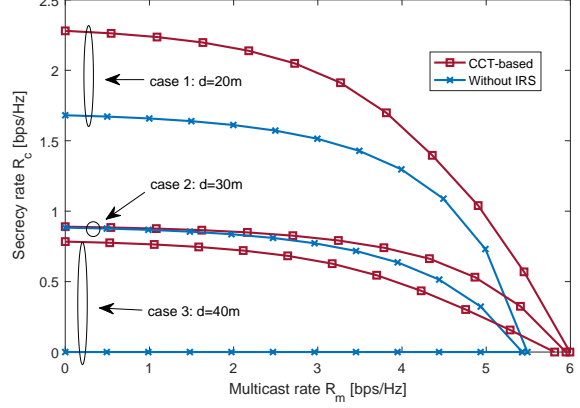


Fig. 5. Secrecy rate regions with different user 1's locations.

CCT-based one, we observe that the performance gap between them is negligible. This indicates that the WSCM-based algorithm can also achieve near-optimal performance, but with lower computational complexity. Next, we compare the proposed algorithm with other benchmarks. As seen in the figure, the Random IRS scheme brings marginal performance gain over the conventional PHY-SI without IRS, while the schemes with optimized IRS PSs (e.g., using the CCT-based and WSCM-based algorithms) are able to achieve remarkable performance gain over it, especially when the desired multicast rate is low and high. The unsatisfying performance of the random IRS scheme matches our theoretical analysis in Section V, i.e., an arbitrary IRS passive beamforming may not improve the performance of PHY-SI. Finally, for the TDMA scheme, it is observed to yield a much worse performance compared to the proposed schemes. This shows the necessity of spectrum sharing for integrating different services.

Fig. 4 compares the secrecy rate regions achieved by different schemes under different transmit powers, namely, $P = 100\text{mW}$, 1W and 10W . It is observed from Fig. 4 that a larger transmit power yields a larger secrecy rate region. As the transmit power increases from 100mW to 10W , the maximum multicast rate increases faster than the maximum secrecy rate in all schemes. By comparing the IRS-assisted schemes with the scheme without IRS, it is observed that the IRS passive beamforming brings pronounced performance gain. In particular, one can observe that the maximum secrecy rate by the CCT-based algorithm with $P = 100\text{mW}$ is even larger than that by traditional non-IRS system with $P = 10\text{W}$. This implies that using IRS can yield better performance even at a lower transmit power. Furthermore, when the desired multicast rate equals to the half of the maximum multicast rate, the performance gap between the CCT-based

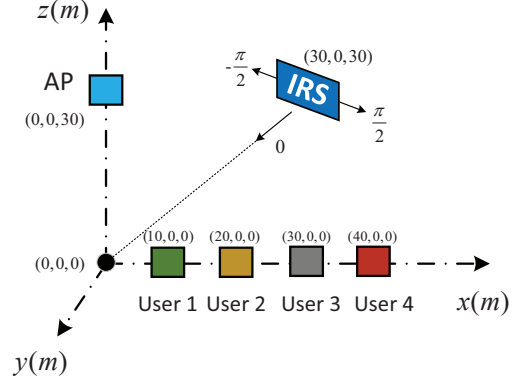
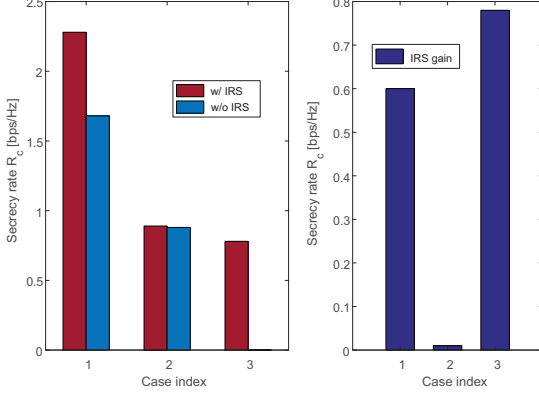


Fig. 6. Maximum secrecy rates and IRS gains in different cases. Fig. 7. Simulation setup of the multi-user system with $K = 4$.

algorithm and TDMA attains its maximum, especially when the transmit power is high.

In Fig. 5, we evaluate the secrecy rate regions by varying the location of user 1, i.e., d_1 . Note that we in this example set $\kappa = 10^3$ to reduce the channel randomness. Cases 1, 2 and 3 correspond to the three locations of user 1 with parameters $d_1 = 20, 30$ and 40 , respectively, as depicted in Fig. 2. Fig. 5 shows that as user 1 moves away from the AP, i.e., d_1 increases, the secrecy rate regions achieved by the CCT-based algorithm and no-IRS system shrink while the reduction in the maximum secrecy rates are much greater than that of the maximum multicast rates. To more clearly explain this observation, Fig. 9 shows the maximum secrecy rates and the performance gap between the above two schemes. It is observed that in case 3, even though the distance between user 1 and the AP is not smaller than that between user 2 and the AP, the secrecy rate is positive in the IRS-assisted system while it is zero in the traditional system. Besides, their performance gap is rather significant in cases 1 and 3 but is negligible in case 2. This is because in case 2, users 1 and 2 are in the same direction from the IRS, which makes it hard to improve the secrecy rate performance as IRS passive beamforming can potentially improve the channel quality of both users simultaneously. This is consistent with our theoretical analysis in Section V.

B. Multi-User Case

Now, we consider the multi-user case with $K = 4$. As shown in Fig. 7, we set the locations of the AP and IRS at $(0, 0, 30)$ and $(30, 0, 30)$, respectively, while the location of the k -th user is located at $(0, 0, 10k)$, $k = 1, 2, 3, 4$. We still compare our proposed algorithms to the above mentioned benchmarks. It is worth mentioning that in the traditional scheme, only the user with

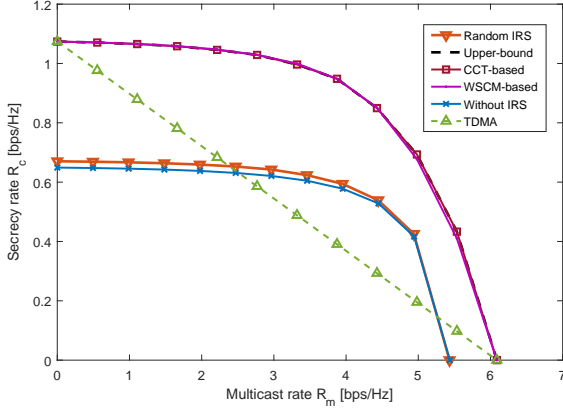


Fig. 8. Secrecy rate regions by different schemes in the multi-user system with $K = 4$.

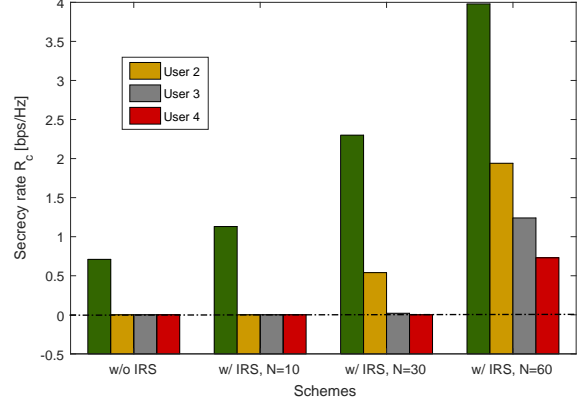


Fig. 9. Maximum secrecy rates at different users.

the shortest distance to AP is able to order confidential information. Due to this fact, user 1 is the legitimate user, while other users are eavesdroppers.

Fig. 8 shows the secrecy rate regions under different schemes in the multi-user scenario. It is observed that the CCT-based algorithm still yields a performance close to the performance upper bound. Moreover, the performance of the random IRS scheme is close to that of the traditional no-IRS system, which implies that only relying on IRS random reflection cannot bring significant performance gain. In contrast, our proposed approaches, i.e., CCT-based and WSCM-based algorithms, strikingly outperform the traditional and TDMA schemes. By comparing Fig. 8 with Fig. 3, we observe that the two figures exhibit a similar trend but the secrecy rate regions in Fig. 8 are smaller. This is due to the fact that the increase in the number of eavesdroppers is detrimental to the secrecy rate, while the QoMS needs to be satisfied for more users.

As previously mentioned, users 2-4 cannot achieve positive secrecy rate in the traditional no-IRS system. However, in the presence of an IRS, the effective legitimate and wiretap channels in the system may be significantly changed, making it possible for other users to achieve positive secrecy rates. To verify this fact, we treat users 2-4 as the legitimate users and compare their respective maximum achievable secrecy rates in the traditional and IRS-assisted schemes in Fig. 9, where the number of IRS reflecting elements is set to $N = 10, 30$ and 60 . From Fig. 9, it is observed that user 1 can achieve positive secrecy rate in both schemes considered and its secrecy rate monotonically increases with the number of IRS reflecting elements. Moreover, in the IRS-assisted scheme with $N = 30$, when user 2 is treated as a legitimate user, although,

although user 1 (eavesdropper) is closest to the AP, user 2 can still achieve a positive secrecy rate thanks to IRS passive beamforming. As N increases to 60, all users are able to achieve positive secrecy rates, which demonstrates that increasing the number of IRS reflecting elements is an effective means to improve the performance of PHY-SI, allowing more users to order the confidential service.

VII. CONCLUSIONS

We studied a joint power allocation and passive beamforming design for an IRS-aided PHY-SI system. Two customized algorithms, i.e., CCT-based algorithm and WSCM-based algorithm, were proposed to approximately characterize the secrecy rate region. Both optimality and complexity analysis of the proposed algorithms were provided, which show that a complexity-performance trade-off can be flexibly balanced by setting the number of sampling points in the uniform search. Furthermore, to gain essential insights, we performed theoretical analysis to reveal how IRS passive beamforming improves the performance of PHY-SI compared to the traditional system without IRS. Numerical results showed that both proposed algorithms achieve near-optimal performance. It is also revealed that the secrecy rate region can be significantly enlarged by the IRS, and that the number of potential users of the confidential service may be increased thanks to the IRS passive beamforming. Finally, our theoretical analysis was also validated via the numerical results. This work can be extended in several promising directions, e.g., in the more general multi-group multicast MISO/MIMO IRS-assisted systems [27]. Besides, it is also interesting to consider multiple IRSs and investigate their joint passive beamforming design [28] and cooperative signal reflection [29].

APPENDIX A

PROOF OF PROPOSITION 1

To determine the feasibility of problem (P1), we need to check whether constraints (4b) and (4c) are feasible or not. As both R_m and R_c are non-negative, we only need to verify whether the LHSs of (4b) and (4c) are no smaller than zero. It is obvious that the LHS of (4b) is always no less than zero for any variables α , β , and \mathbf{v} . Hence, it suffices to check the LHS of (4c). For (4c), it is equivalent to verifying whether there exists an \mathbf{v} , such that the following inequality holds,

$$|\mathbf{m}_1^H \text{diag}(\mathbf{v}^*) \mathbf{g} + h_1|^2 \geq \max_k \frac{\sigma_1^2}{\sigma_k^2} |\mathbf{m}_k^H \text{diag}(\mathbf{v}^*) \mathbf{g} + h_k|^2. \quad (54)$$

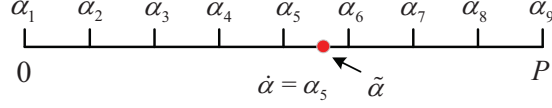


Fig. 10. An illustration of the uniform line search in Algorithm 1 with $T_\alpha = 9$.

Notice that $\mathbf{m}_k^H \text{diag}(\mathbf{v}^*) \mathbf{g} = \sum_{i=1}^N e^{j\theta_i} \mathbf{m}_k^*(i) \mathbf{g}(i)$. The maximum absolute value is achieved when the PSs are selected as $\theta_i = \phi_c - \arg[\mathbf{m}_k^*(i) \mathbf{g}(i)]$ with an arbitrary ϕ_c . Let \mathbf{v}_k be a PS vector with $\mathbf{v}_k(i) = e^{j \arg[\mathbf{m}_k^*(i) \mathbf{g}(i)]}$. If $\left| \sum_{i=1}^N |\mathbf{m}_1(i)| |\mathbf{g}(i)| + h_1 \right|^2 \geq \max_k \frac{\sigma_1^2}{\sigma_k^2} \left| \sum_{i=1}^N |\mathbf{m}_k(i)| |\mathbf{g}(i)| + h_k \right|^2$ holds, there must exist a $\mathbf{v} = \mathbf{v}_1$ that satisfies (54) due to the following relationship,

$$\begin{aligned} |\mathbf{m}_1^H \text{diag}(\mathbf{v}_1^*) \mathbf{g} + h_1|^2 &= \left| \sum_{i=1}^N |\mathbf{m}_1(i)| |\mathbf{g}(i)| + h_1 \right|^2 \geq \max_k \frac{\sigma_1^2}{\sigma_k^2} \left| \sum_{i=1}^N |\mathbf{m}_k(i)| |\mathbf{g}(i)| + h_k \right|^2 \\ &= \max_k \max_{\mathbf{v}} \frac{\sigma_1^2}{\sigma_k^2} |\mathbf{m}_k^H \text{diag}(\mathbf{v}^*) \mathbf{g} + h_k|^2 \geq \max_k \frac{\sigma_1^2}{\sigma_k^2} |\mathbf{m}_k^H \text{diag}(\mathbf{v}_1^*) \mathbf{g} + h_k|^2. \end{aligned} \quad (55)$$

If there exists some k that satisfies $\left| \sum_{i=1}^N |\mathbf{m}_1(i)| |\mathbf{g}(i)| + h_1 \right|^2 \leq \frac{\sigma_1^2 |h_k|^2}{\sigma_k^2}$. We have $\max_k \frac{\sigma_1^2}{\sigma_k^2} |\mathbf{m}_k^H \text{diag}(\mathbf{v}^*) \mathbf{g} + h_k|^2 > |\mathbf{m}_1^H \text{diag}(\mathbf{v}^*) \mathbf{g} + h_1|^2$ for any \mathbf{v} due to the following relationship,

$$\begin{aligned} \max_k \frac{\sigma_1^2}{\sigma_k^2} |\mathbf{m}_k^H \text{diag}(\mathbf{v}^*) \mathbf{g} + h_k|^2 &\geq \frac{\sigma_1^2}{\sigma_k^2} |\mathbf{m}_k^H \text{diag}(\mathbf{v}^*) \mathbf{g} + h_k|^2 > \frac{\sigma_1^2 |h_k|^2}{\sigma_k^2} \\ &\geq \left| \sum_{i=1}^N |\mathbf{m}_1(i)| |\mathbf{g}(i)| + h_1 \right|^2 \geq |\mathbf{m}_1^H \text{diag}(\mathbf{v}^*) \mathbf{g} + h_1|^2, \end{aligned} \quad (56)$$

which contradicts (54). Thus, the two sufficient conditions given in Proposition 1 are needed to verify the feasibility of (P1).

APPENDIX B

PROOF OF PROPOSITION 2

Let $\dot{\alpha}$ represent the sampling point that is smaller than but closest to $\tilde{\alpha}$ (see Fig. 10). Then, we have

$$R_\Delta \triangleq R_c(r_m, \tilde{\alpha}) - \bar{R}_c(r_m) = \log \frac{C(r_m, \tilde{\alpha})}{\max_t C(r_m, \alpha_t)} \leq \log \frac{C(r_m, \tilde{\alpha})}{C(r_m, \dot{\alpha})}. \quad (57)$$

In particular, $C(r_m, \tilde{\alpha})$ can be written as the objective function of $(\hat{\text{P}}10)$ at its optimal solution, i.e., $C(r_m, \tilde{\alpha}) = \text{Tr}[\tilde{\mathbf{Y}}(\frac{\sigma_1^2}{N+1}\mathbf{I} + \tilde{\alpha}\mathbf{T}_1)]$. Let $\delta = \tilde{\alpha} - \dot{\alpha} \geq 0$; thus, $C(r_m, \dot{\alpha})$ can be expressed as

$$C(r_m, \dot{\alpha}) = \max_{\mathbf{Y}, \xi} \text{Tr} \left[\mathbf{Y} \left(\frac{\sigma_1^2}{N+1} \mathbf{I} + (\tilde{\alpha} - \delta) \mathbf{T}_1 \right) \right] \quad (58a)$$

$$\text{s.t. } \text{Tr} \left[\mathbf{Y} \left(\frac{\sigma_1^2}{N+1} \mathbf{I} + \frac{\sigma_1^2}{\sigma_k^2} (\tilde{\alpha} - \delta) \mathbf{T}_k \right) \right] \leq 1, \quad \forall k \in \mathcal{E}, \quad (58b)$$

$$\text{Tr} \left\{ \mathbf{Y} \left[(\text{P} - (\tilde{\alpha} - \delta) 2^{r_m}) \mathbf{T}_k - \frac{(2^{r_m} - 1) \sigma_k^2}{N+1} \mathbf{I} \right] \right\} \geq 0, \quad \forall k \in \mathcal{E}, \quad (58c)$$

$$\text{Tr}(\mathbf{Y} \mathbf{E}_i) = \xi, \quad i = 1, 2, \dots, N+1, \quad \mathbf{Y} \succeq \mathbf{0}, \quad \xi > 0. \quad (58d)$$

Substituting $\tilde{\mathbf{Y}}$ into (58b), we have

$$\text{Tr} \left[\tilde{\mathbf{Y}} \left(\frac{\sigma_1^2}{N+1} \mathbf{I} + \frac{\sigma_1^2}{\sigma_k^2} (\tilde{\alpha} - \delta) \mathbf{T}_k \right) \right] \leq \text{Tr} \left[\tilde{\mathbf{Y}} \left(\frac{\sigma_1^2}{N+1} \mathbf{I} + \frac{\sigma_1^2}{\sigma_k^2} \tilde{\alpha} \mathbf{T}_k \right) \right] \leq 1, \quad (59)$$

where the second inequality is due to the feasibility of $\tilde{\mathbf{Y}}$ in $(\hat{\text{P}}10)$. Similarly, we have

$$\text{Tr} \left\{ \tilde{\mathbf{Y}} \left[(\text{P} - (\tilde{\alpha} - \delta) 2^{r_m}) \mathbf{T}_k - \frac{(2^{r_m} - 1) \sigma_k^2}{N+1} \mathbf{I} \right] \right\} \geq \text{Tr} \left\{ \tilde{\mathbf{Y}} \left[(\text{P} - \tilde{\alpha} 2^{r_m}) \mathbf{T}_k - \frac{(2^{r_m} - 1) \sigma_k^2}{N+1} \mathbf{I} \right] \right\} \geq 0. \quad (60)$$

Thus, $(\tilde{\mathbf{Y}}, \tilde{\xi})$ is a feasible solution to (58). Let $(\dot{\mathbf{Y}}, \dot{\xi})$ be an optimal solution to (58), it holds that

$$\text{Tr}[\dot{\mathbf{Y}}(\frac{\sigma_1^2}{N+1}\mathbf{I} + (\tilde{\alpha} - \delta)\mathbf{T}_1)] \geq \text{Tr}[\tilde{\mathbf{Y}}(\frac{\sigma_1^2}{N+1}\mathbf{I} + (\tilde{\alpha} - \delta)\mathbf{T}_1)]. \quad (61)$$

Based on (57) and (61), we obtain

$$\begin{aligned} R_\Delta &\leq \log \frac{C(r_m, \tilde{\alpha})}{C(r_m, \dot{\alpha})} = \log \frac{\text{Tr}[\tilde{\mathbf{Y}}(\frac{\sigma_1^2}{N+1}\mathbf{I} + \tilde{\alpha}\mathbf{T}_1)]}{\text{Tr}[\dot{\mathbf{Y}}(\frac{\sigma_1^2}{N+1}\mathbf{I} + (\tilde{\alpha} - \delta)\mathbf{T}_1)]} \\ &\leq \log \frac{\text{Tr}[\tilde{\mathbf{Y}}(\frac{\sigma_1^2}{N+1}\mathbf{I} + \tilde{\alpha}\mathbf{T}_1)]}{\text{Tr}[\tilde{\mathbf{Y}}(\frac{\sigma_1^2}{N+1}\mathbf{I} + (\tilde{\alpha} - \delta)\mathbf{T}_1)]} \\ &= \log \left(1 + \frac{\delta \text{Tr}(\tilde{\mathbf{Y}} \mathbf{T}_1)}{\text{Tr}[\tilde{\mathbf{Y}}(\frac{\sigma_1^2}{N+1}\mathbf{I} + (\tilde{\alpha} - \delta)\mathbf{T}_1)]} \right) \leq \log \left(1 + \frac{\delta \text{Tr}(\tilde{\mathbf{Y}} \mathbf{T}_1)}{\tilde{\xi} \sigma_1^2} \right), \end{aligned} \quad (62)$$

where the last inequality holds due to the fact that $\text{Tr}(\tilde{\mathbf{Y}} \mathbf{E}_i) = \tilde{\xi}$, $\forall i$, and we discard the term $(\tilde{\alpha} - \delta) \mathbf{T}_1$ as $\tilde{\alpha} - \delta = \dot{\alpha} \geq 0$. Since both $\tilde{\mathbf{Y}}$ and \mathbf{T}_1 are positive semi-definite matrices, we have the Cauchy-Schwarz inequality, i.e., $\text{Tr}(\tilde{\mathbf{Y}} \mathbf{T}_1) \leq \text{Tr}(\tilde{\mathbf{Y}}) \text{Tr}(\mathbf{T}_1) = \tilde{\xi} (N+1) \text{Tr}(\mathbf{T}_1)$. In addition, δ is the gap between $\tilde{\alpha}$ and $\dot{\alpha}$, which is no larger than the sampling interval of the linear search, i.e., $\delta \leq \frac{P}{T_\alpha - 1}$. As a result, the performance gap can be further upper bounded as

$$R_\Delta \leq \log \left(1 + \frac{\delta \text{Tr}(\tilde{\mathbf{Y}} \mathbf{T}_1)}{\tilde{\xi} \sigma_1^2} \right) \leq \log \left(1 + \frac{\delta (N+1) \text{Tr}(\mathbf{T}_1)}{\sigma_1^2} \right) \leq \log \left(1 + \frac{P(N+1) \text{Tr}(\mathbf{T}_1)}{\sigma_1^2 (T_\alpha - 1)} \right). \quad (63)$$

APPENDIX C

PROOF OF COROLLARY 1

Despite that the difference between (30) and (29) is small, the proof is not straightforward. By leveraging the inequalities given in (57), (62) and (63), we obtain that

$$\log \frac{C(r_m, \tilde{\alpha})}{C(r_m, \alpha_c)} = \log \frac{C(r_m, \tilde{\alpha})}{\max_t C(r_m, \alpha_t)} \leq \log \frac{C(r_m, \tilde{\alpha})}{C(r_m, \dot{\alpha})} \leq \log \left[1 + \frac{P(N+1)\text{Tr}(\mathbf{T}_1)}{\sigma_1^2(T_\alpha - 1)} \right]. \quad (64)$$

In general cases, an SDR solution to (P10) may not be tight with $\alpha = \alpha_c$ and we have $\log[C(r_m, \alpha_c)] = R_c(r_m, \alpha_c) + \Delta_c$. Let $\log[C(r_m, \tilde{\alpha})] = R_c(r_m, \tilde{\alpha}) + \tilde{\Delta}$ with $\tilde{\Delta} \geq 0$. Then, it holds that

$$\begin{aligned} R_\Delta &= R_c(r_m, \tilde{\alpha}) - R_c(r_m, \alpha_c) = \log[C(r_m, \tilde{\alpha})] - \log[C(r_m, \alpha_c)] - \tilde{\Delta} + \Delta_c \\ &\leq \log \left(1 + \frac{P(N+1)\text{Tr}(\mathbf{T}_1)}{\sigma_1^2(T_\alpha - 1)} \right) - \tilde{\Delta} + \Delta_c \leq \log \left(1 + \frac{P(N+1)\text{Tr}(\mathbf{T}_1)}{\sigma_1^2(T_\alpha - 1)} \right) + \Delta_c. \end{aligned} \quad (65)$$

It has been shown that the rank-one solution obtained by the GRP guarantees a worst-case performance ratio of $\frac{\pi}{4}$ to the SDR solution [26], i.e., $\frac{2R_c(r_m, \alpha_c)}{C(r_m, \alpha_c)} \geq \frac{\pi}{4}$. Due to the relation $C(r_m, \alpha_c) = 2^{R_c(r_m, \alpha_c) + \Delta_c}$, we have

$$\frac{C(r_m, \alpha_c)}{2^{R_c(r_m, \alpha_c)}} = 2^{\Delta_c} \leq \frac{4}{\pi}. \quad (66)$$

By substituting (66) into (65), the worst-case performance gap is obtained in (31).

REFERENCES

- [1] C. Liaskos, S. Nie, A. Tsioliaridou, A. Pitsillides, S. Ioannidis, and I. Akyildiz, "A new wireless communication paradigm through softwarecontrolled metasurfaces," *IEEE Commun. Mag.*, vol. 56, no. 9, pp. 162-169, Sep. 2018.
- [2] T. J. Cui, M. Q. Qi, X. Wan, J. Zhao, and Q. Cheng, "Coding Metamaterials, Digital Metamaterials and Programmable Metamaterials," *Light: Science & Applications*, vol. 3, no. 10, pp. e218, Oct. 2014.
- [3] E. Basar, M. D. Renzo, J. de Rosny, M. Debbah, M.-S. Alouini, and R. Zhang, "Wireless communications through reconfigurable intelligent surfaces," *IEEE Access*, vol. 7, pp. 116753-116773, 2019.
- [4] Q. Wu and R. Zhang, "Intelligent Reflecting Surface-Enhanced Wireless Network via Joint Active and Passive Beamforming," *IEEE Trans. Wireless Commun.*, vol. 18, no. 11, pp. 5394-5409, Nov. 2019.
- [5] H. Guo, Y. Liang, J. Chen and E. G. Larsson, "Weighted Sum-Rate Maximization for Reconfigurable Intelligent Surface Aided Wireless Networks," *IEEE Trans. Wireless Commun.* vol. 19, no. 5, pp. 3064-3076, May 2020.
- [6] C. Huang, A. Zappone, G. C. Alexandropoulos, M. Debbah and C. Yuen, "Reconfigurable Intelligent Surfaces for Energy Efficiency in Wireless Communication," *IEEE Trans. Wireless Commun.*, vol. 18, no. 8, pp. 4157-4170, Aug. 2019.
- [7] B. Ning, Z. Chen, W. Chen, and J. Fang, "Beamforming Optimization for Intelligent Reflecting Surface Assisted MIMO: A Sum-Path-Gain Maximization Approach," *IEEE Wireless Commun. Lett.* vol. 9, no. 7, pp. 1105-1109, Jul. 2020.
- [8] S. Zhang and R. Zhang, "Capacity Characterization for Intelligent Reflecting Surface Aided MIMO Communication," *IEEE J. Sel. Areas Commun.*, vol. 38, no. 8, pp. 1823-1838, Aug. 2020.

- [9] P. Wang, J. Fang, L. Dai and H. Li, "Joint Transceiver and Large Intelligent Surface Design for Massive MIMO MmWave Systems," *IEEE Trans. Wireless Commun.* doi: 10.1109/TWC.2020.3030570.
- [10] C. Pan et al., "Multicell MIMO Communications Relying on Intelligent Reflecting Surfaces," *IEEE Trans. Wireless Commun.* vol. 19, no. 8, pp. 5218-5233, Aug. 2020.
- [11] B. Ning, Z. Chen, W. Chen and L. Li, "Improving Security of THz Communication with Intelligent Reflecting Surface," *IEEE Globecom Workshops(GC Wkshps)*, Waikoloa, HI, USA, pp. 1-6, 2019.
- [12] M. Cui, G. Zhang, and R. Zhang, "Secure wireless communication via intelligent reflecting surface," *IEEE Wireless Commun. Lett.*, vol. 8, no. 5, pp. 1410-1414, Oct. 2019.
- [13] H. Shen, W. Xu, S. Gong, Z. He, and C. Zhao, "Secrecy rate maximization for intelligent reflecting surface assisted multi-antenna communications," *IEEE Commun. Lett.*, vol. 23, no. 9, pp. 1488-1492, Sep. 2019.
- [14] J. Chen, Y. Liang, Y. Pei and H. Guo, "Intelligent Reflecting Surface: A Programmable Wireless Environment for Physical Layer Security," *IEEE Access*, vol. 7, pp. 82599-82612, 2019.
- [15] X. Guan, Q. Wu, and R. Zhang, "Intelligent reflecting surface assisted secrecy communication: Is artificial noise helpful or not?" *IEEE Wireless Commun. Lett.*, vol. 9, no. 6, pp. 778-782, Jun. 2020.
- [16] I. Csiszár and J. Körner, "Broadcast channels with confidential messages," *IEEE Trans. Inf. Theory*, vol. IT-24, no. 3, pp. 339-348, May 1978.
- [17] W. Mei, Z. Chen, J. Fang and S. Li, "Physical Layer Service Integration in 5G: Potentials and Challenges," *IEEE Access*, vol. 6, pp. 16563-16575, 2018.
- [18] H. D. Ly, T. Liu, and Y. Liang, "Multiple-input multiple-output Gaussian broadcast channels with common and confidential messages," *IEEE Trans. Inf. Theory*, vol. 56, no. 11, pp. 5477-5487, Oct. 2010.
- [19] R. Wyrembelski and H. Boche, "Physical layer integration of private, common, and confidential messages in bidirectional relay networks," *IEEE Trans. Wireless Commun.*, vol. 11, no. 9, pp. 3170-3179, Sep. 2012.
- [20] W. Mei, Z. Chen, and J. Fang, "Secrecy capacity region maximization in Gaussian MISO channels with integrated services," *IEEE Signal Process. Lett.*, vol. 23, no. 8, pp. 1146-1150, Aug. 2016.
- [21] W. Mei, Z. Chen, L. Li, J. Fang, and S. Li, "On artificial-noise-aided transmit design for multiuser MISO systems with integrated services," *IEEE Trans. Veh. Technol.*, vol. 66, no. 9, pp. 8179-8195, Sep. 2017.
- [22] P. Wang, J. Fang, H. Duan and H. Li, "Compressed Channel Estimation for Intelligent Reflecting Surface-Assisted Millimeter Wave Systems," *IEEE Signal Process. Lett.*, vol. 27, pp. 905-909, May 2020.
- [23] Z. He and X. Yuan, "Cascaded Channel Estimation for Large Intelligent Metasurface Assisted Massive MIMO," *IEEE Wireless Commun. Lett.*, vol. 9, no. 2, pp. 210-214, Feb. 2020.
- [24] B. Ning, Z. Chen, W. Chen, and Y. Du, "Channel estimation and transmission for intelligent reflecting surface assisted THz communications," in *Proc. IEEE Intl. Conf. Commun. (ICC)*, Dublin, Ireland, Jun. 2020.
- [25] M. Grant and S. Boyd, "CVX: MATLAB software for disciplined convex programming," Apr. 2011. [Online]. Available: <http://cvxr.com/cvx>.
- [26] S. Zhang, and Y. Huang, "Complex quadratic optimization and semidefinite programming," *SIAM Journal on Optimization* vol. 16, no. 3, pp. 871-890, 2006.
- [27] G. Zhou, C. Pan, H. Ren, K. Wang and A. Nallanathan, "Intelligent Reflecting Surface Aided Multigroup Multicast MISO Communication Systems," *IEEE Trans. Signal Process.*, vol. 68, pp. 3236-3251, 2020.
- [28] X. Hu, C. Zhong, Y. Zhang, X. Chen and Z. Zhang, "Location Information Aided Multiple Intelligent Reflecting Surface Systems," *IEEE Trans. Commun.*, doi: 10.1109/TCOMM.2020.3020577.
- [29] W. Mei and R. Zhang, "Cooperative Beam Routing for Multi-IRS Aided Communication," *IEEE Wireless Commun. Lett.*, doi: 10.1109/LWC.2020.3034370.